The design of transcription factor-based inhibitors to target Myc: drop the Myc!

Ellenbroek, B.D.

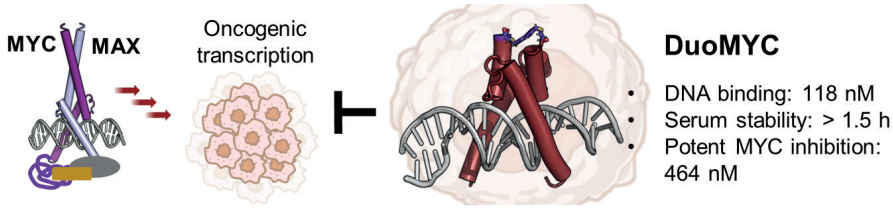

Adapted from: B. D. Ellenbroek, J. P. Kahler, D. Arella, C. Lin, W. Jespers, E. A. Züger, M. Drukker, S. J. Pomplun, "Development of DuoMYC: a synthetic cell penetrant miniprotein that efficiently inhibits the oncogenic transcription factor MYC" *Angewandte Chemie International Edition* **2025**, *64*, DOI 10.1002/anie.202416082.

The data not included in this thesis (uncut gels and list of differently expressed genes) can be found online: https://onlinelibrary.wiley.com/doi/10.1002/anie.202416082

Chapter 3

Development of DuoMYC: A synthetic cell penetrant miniprotein that efficiently inhibits the oncogenic transcription factor MYC

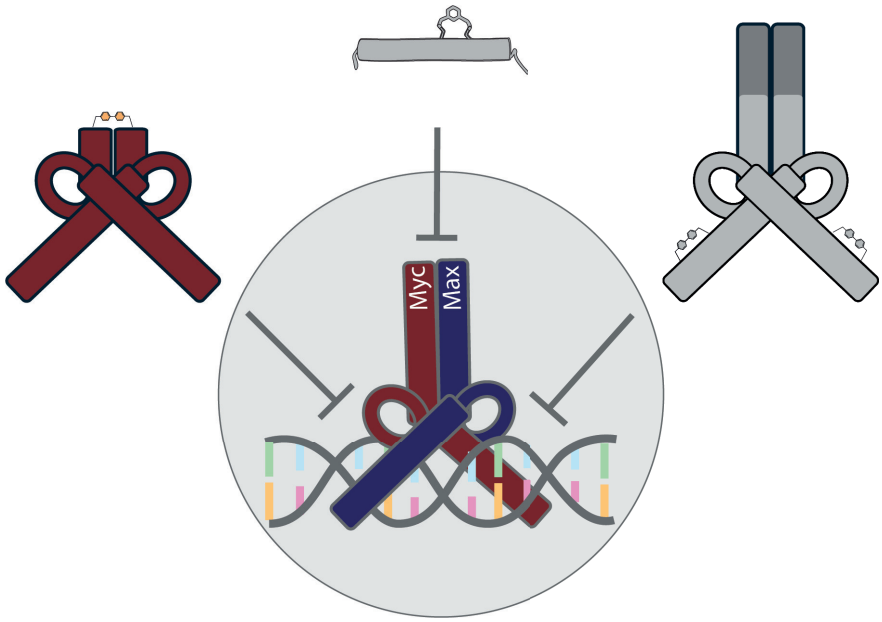

Authors:

Brecht D. Ellenbroek‡, Dr. Jan Pascal Kahler‡, Damiano Arella, Cherina Lin, Dr. Willem Jespers, Eliane Ann-Katrin Züger, Dr. Micha Drukker, Dr. Sebastian J. Pomplun

‡These authors contributed equally.

Abstract

The master regulator transcription factor MYC is implicated in numerous human cancers, and its targeting is a long-standing challenge in drug development. MYC is a typical 'undruggable' target, with no binding pockets on its DNA binding domain and extensive intrinsically disordered regions. Rather than trying to target MYC directly with classical modalities, here we engineer synthetic miniproteins that can bind to MYC's target DNA, the enhancer box (E-Box), and potently inhibit MYC-driven transcription. We crafted the miniproteins via structure-based design and a combination of solid phase peptide synthesis and site-specific crosslinking. Our lead variant, DuoMYC, binds to EBox DNA with high affinity (K_D ~ 0.1 μM) and is able to enter cells and inhibit MYC-driven transcription with submicromolar potency (IC_{50} = 464 nM) as shown by reporter gene assay and confirmed by RNA sequencing. Notably, DuoMYC surpasses the efficacy of several other recently developed MYC inhibitors. Our results highlight the potential of engineered synthetic protein therapeutics for addressing challenging intracellular targets.

3.1 Introduction

Transcription factors (TFs) orchestrate the delicate equilibrium between gene activation and repression and are crucial for cellular function.[1] TFs mainly act via protein-protein and protein-nucleic acid interaction and display extensive intrinsically disordered regions used to recruit components of the transcriptional machinery.[2] These traits make TFs challenging drug targets[3] and highlight the need for innovative approaches in drug discovery and design.

MYC is a prime example of an undruggable TF. It is involved in the pathomechanisms of over 50% of all human cancers.[4–7] To exert its activity, MYC heterodimerizes with its partner MAX and as a complex they bind to enhancer box (E-Box) DNA.[8] MYC's intrinsically disordered transactivation domain (TAD) then recruits the transcriptional machinery and activates gene programs related to cell growth, proliferation and survival.[9] MAX can also homodimerize and occupy the same E-Box sequence as a non-productive inhibitory complex.[10–13] Under healthy conditions MAX/MAX and MYC/MAX are well balanced, while MYC overexpression is involved in many types of cancer. The basic helix-loop-helix leucine zipper motif (bHLH-LZ) of MYC and its intrinsically disordered TAD do not offer any obvious binding sites for inhibitors and no MYC targeted therapeutics are available for patients, to date.

Only recently, a few small molecules with innovative modes of action have shown potential in initial investigations. These include the MAX/MAX stabilizer KI-MS2-008, developed in the Koehler lab,[14] and two compounds inducing MYC instability and degradation: EN4, discovered by Nomura and coworkers,[15] and MYCi361, reported by the group of Abdulkadir.[16] In addition to these approaches, a MYC-targeting bicyclic peptide was recently discovered from a combinatorial library selection.[17]

An intriguing strategy to target MYC is based on the use of proteins that mimic the inhibitory activity of MAX and occupy E-Box DNA.[18–24] However, while protein based modalities generally hold immense potential in targeting 'undruggable' interactions, their usage is usually limited to extracellular targets, because they are unable to cross cell membranes.[25–27] Indeed, also the protein-based MYC inhibitors, of which Omomyc is the most studied representant, have mainly been explored as research tools and utilized via ectopic expression in cells or xenografts.[18,20] However, recently, the Soucek group discovered that purified Omomyc has some intrinsic cell penetrating activity, propelling it from tool compound to a viable therapeutic modality.[28] An Omomyc variant (Omo-103) is currently being investigated in human clinical trials for the treatment of various forms of tumors.[29]

The intrinsic cell penetration of Omomyc makes it a promising therapeutic modality, but at the same time, cell penetration remains its biggest limitation. Wang *et al.,* e.g.,

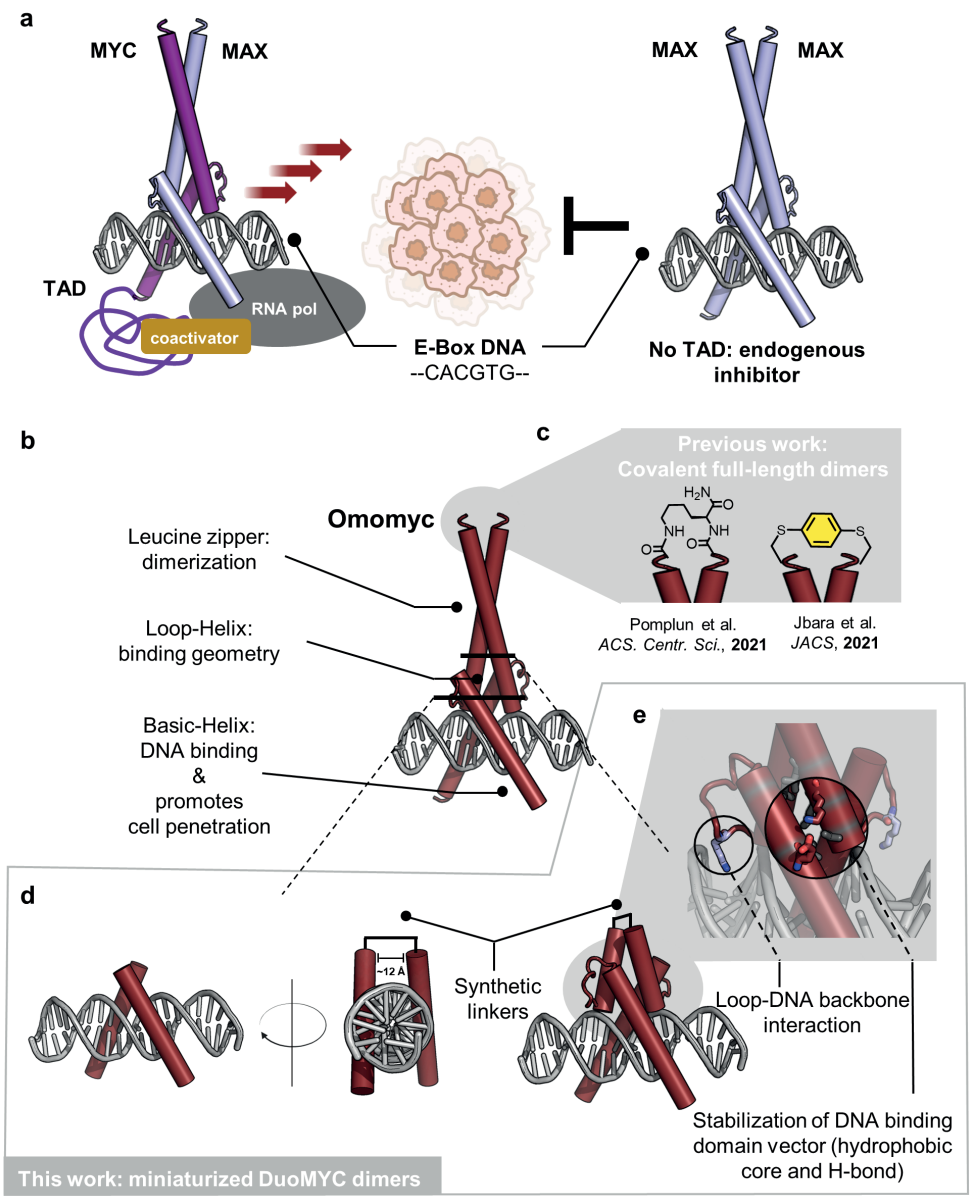

found that Omomyc exhibits negligible cellular uptake unless conjugated to a cell-penetrating modality.[30] These observations correlate well with the fact that, while Omomyc has a low nanomolar binding affinity for E-Box DNA (~25 nM, see **Figure S3.2**), its reported cellular activities are usually 100-1000-fold weaker, when delivered exogenously.[24,28,31,32]

In this study we aim to close this gap and show the development of a synthetic miniprotein that not only has a high affinity for E-Box DNA but, as shown

◀**Figure 3.1 Design of miniaturized protein dimers for MYC inhibition**. a) Schematic representation of MYC's mode of action: MYC upon heterodimerization with MAX binds to E-Box DNA. The MYC-TAD recruits the transcriptional machinery and activates gene transcription. MYC-driven gene programs lead to proliferation, cell growth and survival, all common traits of cancer. MAX can also heterodimerize, occupy the same E-Box DNA and act as an endogenous MYC inhibitor. b) Omomyc is a mutated variant of MYC that can also inhibit MYC by occupying E-Box DNA. c) Recent examples of Omomyc variants with covalently linked dimerization domains. d) Design of a miniaturized E-Box binding dimer, consisting of only the two basic helices of MYC. e) Design of a miniaturized E-Box binding dimer, including the loop helix domain for correct and stable orientation of the basic helices into the major grooves of the E-Box sequence. All structures were generated with Pymol based on PDB 5I50.

by functional cellular assays, can effectively enter cells and inhibit MYC driven transcription with submicromolar potency.

3.2 Results and discussion

To engineer such a bioactive miniprotein, we analyzed the structural features of E-Box binding proteins. The MYC/MAX, MAX/MAX, and Omomyc dimers belong to the bHLH-LZ protein family, where the LZ facilitates dimerization, and the basic helix mediates DNA binding. Dimeric configurations are requisite for DNA interaction, whereas monomers lack such affinity.[31,33] Situated between the basic helix and the LZ, the loop helix domain stabilizes tertiary and quaternary structures, aligning the basic helices appropriately with the major grooves of their target E-Box DNA (**Figure 3.1**). Notably, the basic helix domain drives not only DNA binding but also Omomyc's inherent cell penetration, as evidenced by the loss of this activity upon arginine-to-alanine substitutions within this region.[28]

We reasoned that by miniaturizing Omomyc's structure, we could create a compact dimeric scaffold with improved cell penetration and biological activity. Given the dual role of the basic helix in cell penetration and DNA binding, we envisioned that the development of synthetically dimerized variants of that portion of the protein could lead to optimized MYC inhibitors. The Moellering group recently showed that miniaturized proteomimetics derived from the MAX bHLH domain can tightly bind to E-Box (3.5 nM) and show improved cell penetration compared to full length MAX. [34] However, these compounds required > 1000-fold higher concentrations (20 μM) in order to enable significant effects in cellular assays (e.g. reporter gene). Missing a stable dimerization domain, these compounds might not be able to properly dimerize under physiological conditions inside cells. Similarly, compounds dimerized solely via disulfide linkage are likely to be reduced and to disassemble inside cells.[32,35]

Thus, we here hypothesize that in order to obtain compounds with potent cellular

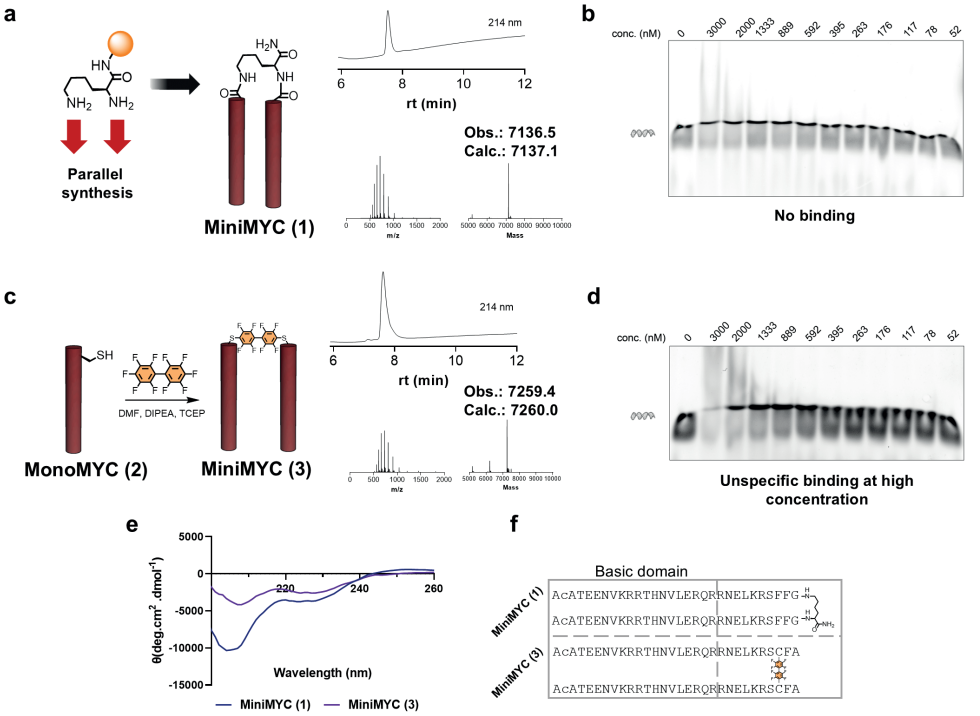

▲Figure 3.2 The basic helix domain of Omomyc is not sufficient for E-Box DNA binding. a) Parallel synthesis of MiniMYC **1** via Fmoc-based SPPS with LCMS analysis of the final product. b) EMSA gel of MiniMYC **1** shows no binding to E-Box DNA. c) Dimerization of MiniMYC **3** with LCMS analysis. d) EMSA gel of MiniMYC **3** shows no binding to E-Box DNA. At high concentration unspecific DNA binding was observed. e) CD spectra of MiniMYC **1** and **3**. f) Sequences of MiniMYC **1** and **3**. General EMSA protocol: labelled dsDNA construct (IRD700-ACCCCACCACGTGGTGCCT, only 5'-strand labelled, final concentration 4 nM) was preincubated with protein in EMSA buffer (20 mM HEPES, pH 8.0, 150 mM NaCl, 5% glycerol, 1 mM EDTA, 2 mM $MgCl_2$, 0.5 mg/mL of BSA, 1 mM DTT and 0.05% NP-40) for 30 minutes at rt followed by 15 minutes on ice and subsequently run on a 10% acrylamide TBE gel under native conditions. General CD protocol: Protein 10/20 μM in 20 mM K_2HPO_4 solution (pH = 7.4) was measured at 37 °C between 190 nm and 260 nm.

activity it is necessary 1) to identify the minimal structure required for specific DNA binding and 2) to covalently link these fragments for a compact and structurally stable scaffold.

We analyzed the DNA bound crystal structure of Omomyc[19] and designed a first miniaturized variant encompassing only the two symmetrical basic helix domains (27 residues). We prepared the dimeric miniMYC **1** via parallel automated solid-phase peptide synthesis (SPPS) using lysine (substituted both on the α- and on the ε-amine) as the covalent linkage between the two chains (**Figure 3.2a**). We first coupled the trifunctional building block Fmoc-Lys(Fmoc)-OH to the solid

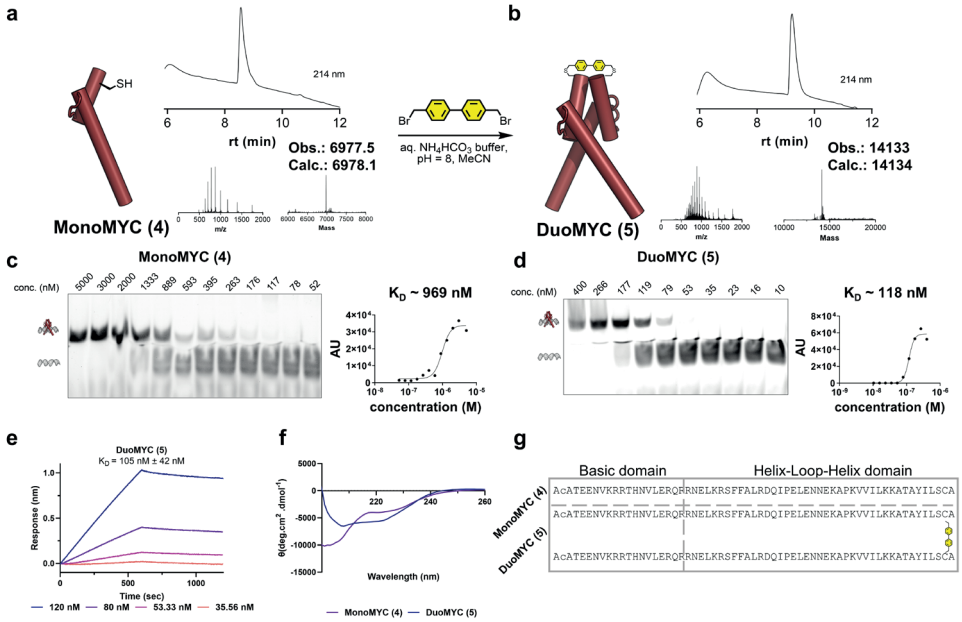

▲Figure 3.3 DuoMYC 5 binds to E-Box DNA with nanomolar affinity. a) LCMS analysis of MonoMYC **4** after SPPS and purification. b) Dimerization of **4** with bis(bromomethyl)biphenyl leads to pure DuoMYC **5** after purification. c) EMSA shows MonoMYC **4** binding to E-Box with a K_D ~ 969 nM. d) EMSA shows DuoMYC **5** binding to E-Box with a K_D ~ 118 nM. e) Binding evaluation by biolayer interferometry shows a K_D of 105 nM for DuoMYC **5**. f) DuoMYC **5** displays the CD spectrum of a partial α-helix while MonoMYC **4** exhibits the one of a random coil with partial helical structure when measured in absence of DNA. g) Sequences of MonoMYC **4** and DuoMYC 5. General SPPS coupling conditions: peptidyl resin incubated with Fmoc-AA-OH (10 eq.), HATU (9 eq.) and DIPEA (29 eq.) in DMF for 8 minutes at 70 °C. Fmoc was removed with 20% piperidine + 2% formic acid in DMF (4 minutes at 70 °C). General EMSA protocol: labelled dsDNA construct (IRD700-ACCCCACCACGTGGTGCCT, final concentration 4 nM) was preincubated with protein in EMSA buffer (20 mM HEPES, pH 8.0, 150 mM NaCl, 5% glycerol, 1 mM EDTA, 2 mM $MgCl_2$, 0.5 mg/mL of BSA, 1 mM DTT and 0.05% NP-40) for 30 minutes at rt followed by 15 minutes on ice and subsequently run on a 10% acrylamide TBE gel under native conditions. General BLI protocol: Protein was dissolved in kinetic buffer (1x PBS, 0.1% BSA, 0.02% Tween-20) with a final volume of 200 µL and measured against a 5' biotinylated hairpin with the sequence: TT CCT CAC GTG GCA TTT GGG TGC CAC GTG AGG. General CD protocol: Protein 10/20 µM in 20 mM K_2HPO_4 solution (pH = 7.4) was measured at 37 °C between 190 nm and 260 nm.

support and, upon removal of both Fmoc protecting groups, we coupled two glycines and performed a parallel synthesis of the 2 x 27mer sequences (**Figure 3.2a**). The Gly-Lys(Gly) linker should effectively bridge the 12 Å distance between the two helices. The dimeric 7 kDa MiniMYC **1** was obtained in good purity, as

shown by LC-MS. However, in electro mobility shift assay (EMSA), we detected no binding between E-Box DNA and MiniMYC **1** (**Figure 3.2b**). We sought to increase the rigidity of the linker for a variant with a stabilized structure, hoping to improve the binding to E-Box DNA. We synthesized monomeric monomer **2** with a Cys close to the C-terminus and linked two monomers using a decafluoro biphenyl reagent. The dimerization reaction worked efficiently and we isolated pure MiniMYC **3** (**Figure 3.2c**). Unfortunately, also this variant did not show any specific association to E-Box DNA (**Figure 3.2d**). For both MiniMYC **1** and **3** circular dichroism (CD) spectra show a partial α-helical structure (**Figure 3.2e**).

We hypothesized that the helix loop domain plays a crucial role in orienting the basic helices into the E-Box major grooves in the correct angle (**Figure 3.1e**). We thus envisioned a medium-sized analog encompassing the helix-loop-helix-domain (HLHD) in addition to the DNA binding helices. Residue 59, just outside the HLHD, appeared as an optimal choice for dimerization with a covalent linker. A direct parallel synthesis of this medium-sized analog failed (data not shown). Therefore, we synthesized a monomeric variant of the 59mer with a single cysteine close to the C-terminus **4** (**Figure 3.3a**). Encouragingly, this medium-sized variant, even without a covalent dimerization linker, exhibited E-Box DNA binding with an affinity of ~969 nM measured by EMSA (**Figure 3.3c**). The loop-helix domain might thus drive protein dimerization, at least to some extent, in good agreement with previous reports.[36] Recognizing, however, that the full-length Omomyc dimerization is mainly driven by the leucine zipper domain which we removed, we again decided to introduce a covalent linker for enhanced structural reinforcement. We cross-linked the two monomers with a bis(bromomethyl)biphenyl linker and successfully generated the synthetic 14 kDa miniprotein dimer, DuoMYC **5** (**Figure 3.3b**). Notably, DuoMYC **5** displayed improved E-Box DNA binding, with a K_D of ~118 nM measured by EMSA (**Figure 3.3d**) and 105 nM measured by biolayer interferometry (**Figure 3.3e, Figures S3.3**), representing an 8-fold enhancement over the monomeric variant. The CD spectrum of DuoMYC **5** shows clear α-helical patterns with defined minima at 208 and 222 nm. We also prepared a second variant, DuoMYC **7**, using a decafluorobiphenyl reagent for dimerization, and obtained a K_D of ~174 nM (**see Figure S3.1** for synthesis details and EMSA, **Figure S3.4** for BLI data). While we do not have a structural proof of DuoMYC's four helix core structure, its strong binding affinity for the E-Box domain and the recently solved structure of a similar miniprotein based on MAX[36] point towards this functional fold.

We next compared the stability of the full length Omomyc/Omomyc-DNA complex with the DuoMYC **5**-DNA complex using molecular dynamic (MD) simulations. The MD simulation was performed using Schrödinger's Desmond using the OPLS4 force field under the NPγT ensemble. Each system was run in triplicates, generating simulations of 500 ns. We found that both Omomyc and DuoMYC **5** remain in a stable DNA bound conformation in each of the three replicate systems, with overall residue fluctuations

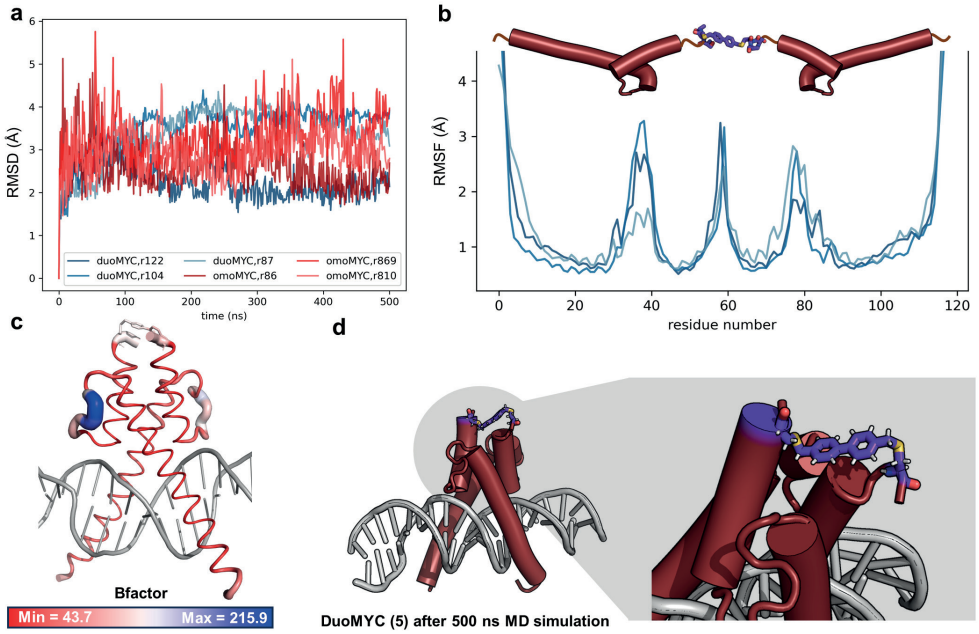

▲Figure 3.4 MD simulation shows stability of DuoMYC 5 DNA complex. a) Root-mean-square-deviation (RMSD) plot of DuoMYC **5** and Omomyc, in blue and red, respectively. Each triplicate simulation was run for 500 ns. b) RMSF plot for DuoMYC 5. c) RMSF plot translated to b-factor and shown as putty representation. d) DuoMYC **5** structure after 500 ns MD simulation with linker region highlighted.

between 2.2 and 3.5 Å compared with their starting coordinates (**Figure 3.4a**).The root-mean-square-fluctuation (RMSF) plot evidences the structural rigidity of the two helical domains in DuoMYC **5**, while the loop connecting the basic helix to the C-terminal helix displays significantly stronger fluctuations (**Figure 3.4b**). A very similar trend could be observed in Omomyc (**Figure S3.5**). The flexibility of the C-terminal extremities of the DuoMYC **5** dimer enables the correct arrangement of the covalent biphenyl linker, connecting the two helices (**Figure 3.4c-d**). Overall, the MD simulation highlights how the compact covalent linker (MW < 200) can efficiently replace the extensive leucine zipper domain (MW > 7000), still resulting in a stable DNA binding scaffold.

Since proteolytic instability is one of the major limitations of peptide-based therapeutics we next assessed the half-life of MonoMYC **4** and DuoMYC **5** in human serum, in comparison to Omomyc. We incubated the compounds in human serum and measured their stability by LC-MS at different timepoints normalizing to an internal standard. MonoMYC **4** was rapidly degraded with an overall half-life of 0.6 hours. DuoMYC **5** in turn, presented an improved stability with 50% compound still intact after 1.8 hours (**Figure 3.5a**), approximately two times longer than Omomyc

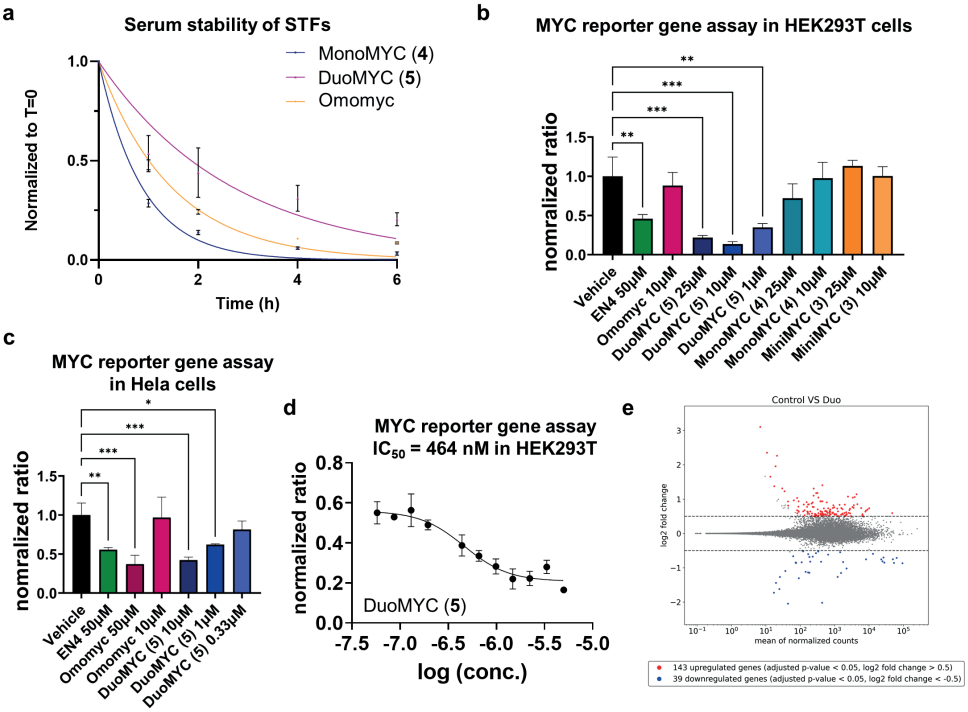
a
Serum stability of STFs
MonoMYC (4)
DuoMYC (5)
Omomyc
Normalized to T=0
Time (h)
b
MYC reporter gene assay in HEK293T cells
nomralized ratio
Vehicle
EN4 50µM
Omomyc 10µM
DuoMYC (5) 25µM
DuoMYC (5) 10µM
DuoMYC (5) 1µM
MonoMYC (4) 25µM
MonoMYC (4) 10µM
MiniMYC (3) 25µM
MiniMYC (3) 10µM
c
MYC reporter gene assay in Hela cells
nomralized ratio
Vehicle
EN4 50µM
Omomyc 50µM
Omomyc 10µM
DuoMYC (5) 10µM
DuoMYC (5) 1µM
DuoMYC (5) 0.33µM
d
MYC reporter gene assay
IC50 = 464 nM in HEK293T
normalized ratio
DuoMYC (5)
log (conc.)
e
Control VS Duo
log2 fold change
mean of normalized counts
143 upregulated genes (adjusted p-value < 0.05, log2 fold change > 0.5)
39 downregulated genes (adjusted p-value < 0.05, log2 fold change < -0.5)

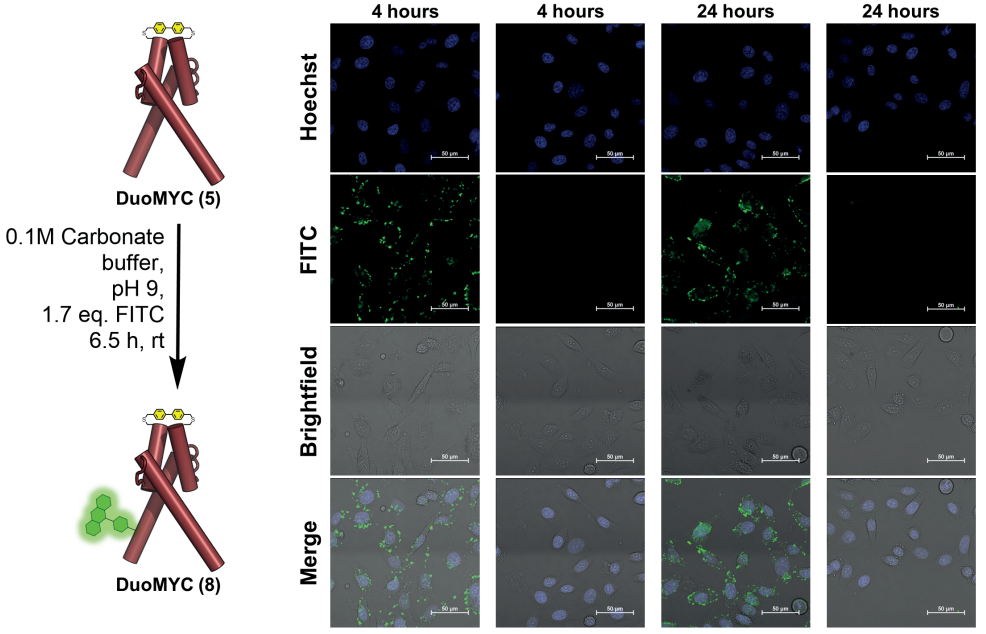
f
DuoMYC (5)
0.1M Carbonate buffer, pH 9, 1.7 eq. FITC 6.5 h, rt
DuoMYC (8)
g
1 µM DuoMYC (8) 4 hours
1 µM Omomyc (9) 4 hours
1 µM DuoMYC (8) 24 hours
1 µM Omomyc (9) 24 hours
Hoechst
FITC
Brightfield
Merge

◂Figure 3.5 DuoMYC 5 inhibits MYC driven transcription with submicromolar potency and displays good serum stability and cell penetration. a) MonoMYC **4** displays a half-life of 0.6 hours, DuoMYC **5** a half-life of 1.8 hours and Omomyc a half-life of 1 hour. General serum stability protocol: proteins were dissolved in 10% human serum in DPBS to a final concentration of 60 µM, mixed and after the indicated time aliquots were taken and inactivated with 20% TFA in H_2O. The samples were analyzed via high-resolution LC-MS and curves plotted in Graphpad Prism 9. The standard deviations plotted are from n = 3 independent samples. b,c) MYC reporter gene assay with single concentrations of several compounds. HEK293T (b) or Hela (c) cells were transfected with a dual reporter gene, containing a MYC dependent firefly luciferase gene and a MYC independent, constitutively expressing renilla luciferase construct. The cells were treated with compounds at the indicated concentrations for 24 h. Subsequently, the cells were lysed, luciferase luminescence measured and the data were normalized to the control. Statistical significance details: one-way ANOVA was performed and revealed that there was a statistically significant difference in MYC-responsive luminescence between at least two groups (b) $F(9, 14) = 12.65$, $p < 0.0001$; (c) $F(6, 14) = 11.33$, $p < 0.0001$. Dunnett's multiple comparisons test was performed to test for a significant difference of the various groups from vehicle. * $p<0.05$, ** $p<0.01$, *** $p<0.001$. d) Concentration curve of DuoMYC **5** reporter gene activity in transfected HEK293T cells. Curve shown is one of three independent experiments (see **Figure S3.6** for all experiments). e) RNA sequencing of HCT116 cells reveals that 182 genes were differently expressed compared to the non-treated cells. (f) DuoMYC **5** was reacted with FITC in carbonate buffer to yield unspecifically fluorescein-labelled DuoMYC **8**. (g) Confocal microscopy images show cell penetration of DuoMYC **8**. Hela cells were treated with 1 µM DuoMYC **8** or 1 µM FITC-labelled Omomyc for 24 h or 4 h and images of live cells acquired after washing. Hoechst dye was used for nuclear staining. Images shown were stitched from four acquired images.

(**Figure 3.5a, Figure S3.7**). The higher stability could be related to the fact that the crosslinked, dimeric scaffold is less accessible to proteases.

To assess whether the tight binding activity and the miniaturized, stable structure of DuoMYC **5** would translate to improved biological *in cell* activity we performed a MYC reporter gene assay. The reporter is based on a firefly luciferase gene activatable by MYC/MAX-dimers. A second constitutively-expressing Renilla luciferase vector serves as an internal positive control for normalization. We transfected HEK293T as well as HeLa cells with the reporter gene DNA and treated them with our compounds for 24 h (**Figure 3.5b-c**). Besides DuoMYC **5**, we included the recently discovered covalent small molecule MYC inhibitor EN4 as a positive control for MYC inhibition as it had shown activity in the same assay format.[15] We additionally included recombinant Omomyc (see SI 4.2-4.6 for expression protocol and **Figure S3.2** for EMSA validation) and in HEK293T cells also MniMYC **3** and MonoMYC **4**. In HEK293T cells only EN4 and DuoMYC **5** treatments resulted in statistically significant reduction of MYC-dependent transcription (**Figure 3.5b**). While 50 µM EN4 reduced MYC transcription by ~ 50%, DuoMYC **5** showed stronger inhibition even at 50-fold lower concentration (1 µM). Omomyc did not show any effect on MYC transcription in HEK293T cells. In HeLa cells Omomyc caused significant

reduction of MYC transcription only at its highest concentration (50 μM, **Figure 3.5c**). We next measured a full concentration curve of DuoMYC **5** and determined an IC_{50} of 464 nM in HEK293T (**Figure 3.5d, Figure S3.6**). The MYC-independent control reporter showed a stable signal over the whole concentration range of DuoMYC **5**, indicating that the compound is likely specifically inhibiting MYC driven transcription, rather than non-specifically shutting down cellular gene transcription.

To further assess DuoMYC **5**'s activity under more native conditions, we performed RNA-sequencing on HCT116 cells treated with either DuoMYC **5** (5 μM) or Omomyc (10 μM) for 24 hours, followed by whole RNA isolation. RNA-sequencing of DuoMYC-treated samples, compared to untreated controls, revealed 182 differentially expressed genes (**Figure 3.5e**). Gene set enrichment analysis (GSEA) using the Molecular Signatures Database (MSigDB)[37] identified several significantly modulated pathways, many of which are related to MYC activity and cancer biology. Notably, pathways such as apoptosis, hypoxia, and the G2-M checkpoint were among those significantly impacted, underscoring DuoMYC's role in modulating critical cellular processes that are typically influenced by MYC. The full list of modulated gene sets is provided in Supplementary Information (**Figures 3.S9-17, Table S3.1-4**). Additionally, a significant overlap in differentially expressed genes was observed between DuoMYC and Omomyc treatments (**Figure S3.17**), indicating their common mechanisms of action. We next wanted to confirm and visualize DuoMYC **5**'s uptake into cells. We prepared FITC labeled variants of DuoMYC **5** and Omomyc (**Figure 3.5f**). We then treated Hela cells with either 1 μM or 5 μM FITC-DuoMYC **8** or FITC-Omomyc **9** for 4 has well as 24 h, washed cells and acquired confocal microscopy images of live cells. Already at 1 μM DuoMYC **8** displays clear cellular uptake after 4 h as well as after 24 h treatment. Omomyc **9** at this concentration hardly shows any cell penetration at both treatment times (**Figure 3.5g**, second set of images in **Figure S3.8a**). The same effect with seemingly higher cellular uptake can be seen when cells are treated with 5 μM protein (**Figure S3.8b, Figure S3.8c-d** for untreated cells).

3.3 Conclusion

Taken together, here we have shown the development of a synthetic miniprotein that can bind E-Box DNA with high affinity and inhibit MYC-driven oncogenic transcription. Although MYC is a long sought after drug target, classical small molecule drugs cannot efficiently target MYC because of its lack of binding pockets. At the same time, protein drugs have limited activity due to their poor cell permeability. Our engineered miniprotein DuoMYC **5** combines a strong binding affinity and potent activity in cell assays. Furthermore DuoMYC **5** exhibits promising serum stability. We rationally engineered DuoMYC **5** based on the crystal structure of a larger E-Box targeting modality, Omomyc.[19] Surprisingly, our initial efforts to miniaturize the structure toward a dimeric miniprotein containing only the DNA

binding helices of Omomyc was unsuccessful while similar approaches had shown success in miniaturized GCN4 mimetics.[38,39] The mandatory components for our lead compound include the DNA binding helices, the loop-helix domains and a stable covalent linkage. This scaffold ultimately resulted in an efficient MYC inhibitor. Given the interest in MYC as a cancer drug target,[40] DuoMYC **5** can be considered a highly promising modality. Furthermore, our results highlight the possibility of designing innovative chemical modalities, such as synthetic miniproteins, able to address challenging intracellular targets.

3.4 References

[1] T. I. Lee, R. A. Young, "Transcriptional regulation and its misregulation in disease" *Cell* **2013**, *152*, 1237–1251.

[2] A. Boija, I. A. Klein, B. R. Sabari, A. Dall'Agnese, E. L. Coffey, A. V Zamudio, C. H. Li, K. Shrinivas, J. C. Manteiga, N. M. Hannett, B. J. Abraham, L. K. Afeyan, Y. E. Guo, J. K. Rimel, C. B. Fant, J. Schuijers, T. I. Lee, D. J. Taatjes, R. A. Young, "Transcription Factors Activate Genes through the Phase-Separation Capacity of Their Activation Domains" *Cell* **2018**, *175*, 1842-1855.e16.

[3] J. H. Bushweller, "Targeting transcription factors in cancer — from undruggable to reality" *Nat Rev Cancer* **2019**, *19*, 611–624.

[4] N. Meyer, L. Z. Penn, "Reflecting on 25 years with MYC" *Nat Rev Cancer* **2008**, *8*, 976–990.

[5] S. K. Madden, A. D. de Araujo, M. Gerhardt, D. P. Fairlie, J. M. Mason, "Taking the Myc out of cancer: toward therapeutic strategies to directly inhibit c-Myc" *Mol Cancer* **2021**, *20*, 1–18.

[6] S. K. Das, B. A. Lewis, D. Levens, "MYC: a complex problem" *Trends Cell Biol* **2023**, *33*, 235–246.

[7] B. Ellenbroek, J. P. Kahler, S. R. Evers, S. J. Pomplun, "Synthetic Peptides: Promising Modalities for the Targeting of Disease-Related Nucleic Acids" *Angewandte Chemie (International Edition in English)* **2024**, DOI 10.1002/anie.202401704.

[8] E. M. Blackwood, R. N. Eisenman, "Max: A helix-loop-helix zipper protein that forms a sequence-specific DNA-binding complex with Myc" *Science (1979)* **1991**, *251*, 1211–1217.

[9] M. Kalkat, D. Resetca, C. Lourenco, P. K. Chan, Y. Wei, Y. J. Shiah, N. Vitkin, Y. Tong, M. Sunnerhagen, S. J. Done, P. C. Boutros, B. Raught, L. Z. Penn, "MYC Protein Interactome Profiling Reveals Functionally Distinct Regions that Cooperate to Drive Tumorigenesis" *Mol Cell* **2018**, *72*, 836-848.e7.

[10] E. M. Blackwood, R. N. Eisenman, "Max : A Helix-Loop-Helix Zipper Protein That Complex with Myc" *Science (1979)* **1991**, *251*, 1211–1217.

[11] R. V. Nithun, Y. M. Yao, X. Lin, S. Habiballah, A. Afek, M. Jbara, "Deciphering the Role of the Ser-Phosphorylation Pattern on the DNA-Binding Activity of Max Transcription Factor Using Chemical Protein Synthesis" *Angewandte Chemie - International Edition* **2023**, *62*, DOI 10.1002/anie.202310913.

[12] A. R. Ferré-D'Amaré, G. C. Prendergast, E. B. Ziff, S. K. Burley, "Recognition by Max of its cognate DNA through a dimeric b/HLH/Z domain" *Nature* **1993**, *363*, 38–45.

[13] S. K. Nair, S. K. Burley, "X-ray structures of Myc-Max and Mad-Max recognizing DNA: Molecular bases of regulation by proto-oncogenic transcription factors" *Cell* **2003**, *112*, 193–205.

[14] N. B. Struntz, A. Chen, A. Deutzmann, R. M. Wilson, E. Stefan, H. L. Evans, M. A. Ramirez, T. Liang, F. Caballero, M. H. E. Wildschut, D. V Neel, D. B. Freeman, M. S. Pop, M. McConkey, S. Muller, B. H. Curtin, H. Tseng, K. R. Frombach, V. L. Butty, S. S. Levine, C. Feau, S. Elmiligy, J. A. Hong, T. A. Lewis, A. Vetere, P. A. Clemons, S. E. Malstrom, B. L. Ebert, C. Y. Lin, D. W. Felsher, A. N. Koehler, "Stabilization of the Max Homodimer with a Small Molecule Attenuates Myc-Driven Transcription" *Cell Chem Biol* **2019**, *26*, 711-723.e14.

[15] L. Boike, A. G. Cioffi, F. C. Majewski, J. Co, N. J. Henning, M. D. Jones, G. Liu, J. M. McKenna, J. A. Tallarico, M. Schirle, D. K. Nomura, "Discovery of a Functional Covalent Ligand Targeting an Intrinsically Disordered Cysteine within MYC" *Cell Chem Biol* **2020**, 1–10.

[16] H. Han, A. D. Jain, M. I. Truica, J. Izquierdo-Ferrer, J. F. Anker, B. Lysy, V. Sagar, Y. Luan, Z. R. Chalmers, K. Unno, H. Mok, R. Vatapalli, Y. A. Yoo, Y. Rodriguez, I. Kandela, J. B. Parker, D. Chakravarti, R. K. Mishra, G. E. Schiltz, S. A. Abdulkadir, "Small-Molecule MYC Inhibitors Suppress Tumor Growth and Enhance Immunotherapy" *Cancer Cell* **2019**, *36*, 483-497.e15.

[17] Z. Li, Y. Huang, T. I. Hung, J. Sun, D. Aispuro, B. Chen, N. Guevara, F. Ji, X. Cong, L. Zhu, S. Wang, Z. Guo, C. Chang, M. Xue, "MYC-Targeting Inhibitors Generated from a Stereodiversified Bicyclic Peptide Library" **2023**, DOI 10.1021/jacs.3c09615.

[18] L. Soucek, M. Helmer-Citterich, A. Sacco,

R. Jucker, G. Cesareni, S. Nasi, "Design and properties of a Myc derivative that efficiently homodimerizes" *Oncogene* **1998**, *17*, 2463–2472.

[19] L. A. Jung, A. Gebhardt, W. Koelmel, C. P. Ade, S. Walz, J. Kuper, B. Von Eyss, S. Letschert, C. Redel, L. D'Artista, A. Biankin, L. Zender, M. Sauer, E. Wolf, G. Evan, C. Kisker, M. Eilers, "OmoMYC blunts promoter invasion by oncogenic MYC to inhibit gene expression characteristic of MYC-dependent tumors" *Oncogene* **2017**, *36*, 1911–1924.

[20] L. C. Lustig, D. Dingar, W. B. Tu, C. Lourenco, M. Kalkat, I. Inamoto, R. Ponzielli, W. C. W. Chan, J. A. Shin, L. Z. Penn, "Inhibiting MYC binding to the E-box DNA motif by ME47 decreases tumour xenograft growth" *Oncogene* **2017**, *36*, 6830–6837.

[21] M. Montagne, N. Beaudoin, D. Fortin, C. L. Lavoie, R. Klinck, P. Lavigne, "The max b-HLH-LZ can transduce into cells and inhibit c-Myc transcriptional activities" *PLoS One* **2012**, *7*, 2–10.

[22] X. Lin, O. Harel, M. Jbara, "Chemical Engineering of Artificial Transcription Factors by Orthogonal Palladium(II)-Mediated S-Arylation Reactions" *Angewandte Chemie - International Edition* **2023**, *202317511*, DOI 10.1002/anie.202317511.

[23] S. Pomplun, M. Jbara, C. K. Schissel, S. Wilson Hawken, A. Boija, C. Li, I. Klein, B. L. Pentelute, "Parallel Automated Flow Synthesis of Covalent Protein Complexes That Can Inhibit MYC-Driven Transcription" *ACS Cent Sci* **2021**, *7*, 1408–1418.

[24] M. Jbara, S. Pomplun, C. K. Schissel, S. W. Hawken, A. Boija, I. Klein, J. Rodriguez, S. L. Buchwald, B. L. Pentelute, "Engineering Bioactive Dimeric Transcription Factor Analogs via Palladium Rebound Reagents" *J Am Chem Soc* **2021**, *143*, 11788–11798.

[25] O. Harel, M. Jbara, "Chemical Synthesis of Bioactive Proteins" *Angewandte Chemie - International Edition* **2023**, *62*, DOI 10.1002/anie.202217716.

[26] Leader B, Baca Q J, Golan D E, "Protein therapeutics: a summary and pharmacological classification" *Nat Rev Drug Discov* **2008**, *7*, 21–39.

[27] B. Khatri, I. Pramanick, S. K. Malladi, R. S. Rajmani, S. Kumar, P. Ghosh, N. Sengupta, R. Rahisuddin, N. Kumar, S. Kumaran, R. P. Ringe, R. Varadarajan, S. Dutta, J. Chatterjee, "A dimeric proteomimetic prevents SARS-CoV-2 infection by dimerizing the spike protein" *Nat Chem Biol* **2022**, *18*, 1046–1055.

[28] M. E. Beaulieu, T. Jauset, D. Massó-Vallés, S. Martínez-Martín, P. Rahl, L. Maltais, M. F. Zacarias-Fluck, S. Casacuberta-Serra, E. S. Del Pozo, C. Fiore, L. Foradada, V. C. Cano, M. Sánchez-Hervás, M. Guenther, E. R. Sanz, M. Oteo, C. Tremblay, G. Martín, D. Letourneau, M. Montagne, M. Á. M. Alonso, J. R. Whitfield, P. Lavigne, L. Soucek, "Intrinsic cell-penetrating activity propels omomyc from proof of concept to viable anti-myc therapy" *Sci Transl Med* **2019**, *11*, 1–14.

[29] E. Garralda, M. E. Beaulieu, V. Moreno, S. Casacuberta-Serra, S. Martínez-Martín, L. Foradada, G. Alonso, D. Massó-Vallés, S. López-Estévez, T. Jauset, E. Corral de la Fuente, B. Doger, T. Hernández, R. Perez-Lopez, O. Arqués, V. Castillo Cano, J. Morales, J. R. Whitfield, M. Niewel, L. Soucek, E. Calvo, "MYC targeting by OMO-103 in solid tumors: a phase 1 trial" *Nat Med* **2024**, DOI 10.1038/s41591-024-02805-1.

[30] E. Wang, A. Sorolla, P. T. Cunningham, H. M. Bogdawa, S. Beck, E. Golden, R. E. Dewhurst, L. Florez, M. N. Cruickshank, K. Hoffmann, R. M. Hopkins, J. Kim, A. J. Woo, P. M. Watt, P. Blancafort, "Tumor penetrating peptides inhibiting MYC as a potent targeted therapeutic strategy for triple-negative breast cancers" *Oncogene* **2019**, *38*, 140–150.

[31] S. Pomplun, M. Jbara, C. K. Schissel, S. Wilson Hawken, A. Boija, C. Li, I. Klein, B. L. Pentelute, "Parallel Automated Flow Synthesis of Covalent Protein Complexes That Can Inhibit MYC-Driven Transcription" *ACS Cent Sci* **2021**, *7*, 1408–1418.

[32] Z. Z. Brown, C. Mapelli, I. Farasat, A. V Shoultz, S. A. Johnson, F. Orvieto, A. Santoprete, E. Bianchi, A. B. McCracken, K. Chen, X. Zhu, M. J. Demma, B. M. Lacey, K. A. Canada, R. M. Garbaccio, J. O'Neil, A. Walji, "Multiple Synthetic Routes to the Mini-Protein Omomyc and Coiled-Coil Domain Truncations" *Journal of Organic Chemistry* **2020**, *85*, 1466–1475.

[33] J. G. Kwok, Z. Yuan, P. S. Arora, "An Encodable Scaffold for Sequence-Specific Recognition of Duplex RNA" *Angewandte Chemie International Edition* **2023**, e202308650.

[34] T. E. Speltz, Z. Qiao, C. S. Swenson, X. Shangguan, J. S. Coukos, C. W. Lee, D. M. Thomas, J. Santana, S. W. Fanning, G. L. Greene, R. E. Moellering, "Targeting MYC with modular synthetic transcriptional repressors derived from bHLH DNA-binding domains" *Nat Biotechnol* **2023**, *41*, DOI 10.1038/s41587-022-01504-x.

[35] N. M. McLoughlin, M. A. Albers, E. Collado Camps, J. Paulus, Y. A. Ran, S. Neubacher, S. Hennig, R. Brock, T. N. Grossmann, "Environment-Responsive Peptide Dimers Bind and Stabilize Double-Stranded RNA" *Angewandte Chemie International Edition* **2023**, DOI 10.1002/ANIE.202308028.

[36] T. E. Speltz, Z. Qiao, C. S. Swenson, X. Shangguan, J. S. Coukos, C. W. Lee, D. M. Thomas, J. Santana, S. W. Fanning, G. L. Greene, R. E. Moellering, "Targeting MYC with modular synthetic transcriptional repressors derived from bHLH DNA-binding domains" *Nat Biotechnol* **2023**, *41*, DOI 10.1038/s41587-022-01504-x.

[37] A. Liberzon, C. Birger, H. Thorvaldsdóttir, M. Ghandi, J. P. Mesirov, P. Tamayo, "The Molecular Signatures Database Hallmark Gene Set Collection" *Cell Syst* **2015**, *1*, 417–425.

[38] B. Cuenoud, A. Schepartz, "Altered Specificity of DNA-Binding Proteins with Transition Metal Dimerization Domains" *Science (1979)* **1993**, *259*.

[39] J. Mosquera, M. I. Sánchez, M. E. Vázquez, J. L. Mascareñas, "Ruthenium bipyridyl complexes as photocleavable dimerizers: Deactivation of dna-binding peptides using visible light" *Chemical Communications* **2014**, *50*, 10975–10978.

[40] D. Massó-Vallés, L. Soucek, "Blocking Myc to Treat Cancer: Reflecting on Two Decades of Omomyc" *Cells* **2020**, *9*, 883.

3.5 Experimental

3.5.1 Synthesis procedures

3.5.1.1 Automated solid phase peptide synthesis (SPPS) – general protocol

All peptides were prepared on a Syro I XP synthesizer. The synthesis was performed on Chemmatrix rink amide resin (typically 100 mg, loading capacity of 0.41 mmol/g, 41 µmol scale). The synthesizer was charged with Fmoc-protected amino acid (Fmoc-AA-OH) solutions (0.5 M in DMF), HATU (0.45 M in DMF), Fmoc removal cocktail (20%/2%/78% = piperidine/formic acid/DMF) and pure DIPEA. As the first step in the peptide synthesis, the peptidyl resin was incubated at 70 °C in DMF while shaking for 10 min, after which the following coupling cycle was repeated until completion of the synthesis:

Coupling cycle

Coupling: Fmoc-AA-OH (10 eq., 800 µL for the 41 µmol scale), HATU (9 eq., 800 µL for the 41 µmol scale) and DIPEA (28.7 eq., 100 uL for the 41 umol scale) were sequentially added to the peptidyl resin and incubated at 70 °C for 8 minutes, with vigorous interval vortexing, followed by vacuum based draining of the resin.

Washing: DMF (1.2 mL) was added to the peptidyl resin, incubated for 1 min at room temperature (RT) with vigorous vortexing followed by vacuum based draining of the resin. The step was repeated 3 times.

Fmoc removal: Fmoc removal cocktail (1.5 mL) was added to the peptidyl resin incubated at 70 °C for 4 minutes, with vigorous interval vortexing.

Washing: DMF (1.2 mL) was added to the peptidyl resin, incubated for 1 min at RT with vigorous vortexing followed by vacuum based draining of the resin. The step was repeated 3 times.

After completion, the peptidyl resin was washed with DMF (3x), DCM (3x), dried under vacuum and either stored at -20 ˚C or directly acetylated.

3.5.1.2 Acetylation

After completion of the SPPS, the peptides were acetylated. First, the dry peptidyl resin was swollen in DMF (10 min) and subsequently vacuum-based drained. To the DMF soaked peptidyl resin the acetylation mixture (10%/10%/80% = Ac_2O/DIPEA/DMF) was administered (3 mL for 41 µL scale). The resin was thorougly shaken for 15 min at RT. The resin was subsequently washed with DMF (3x), DCM (3x), dried

under vacuum and either stored at -20 ˚C or cleaved immediately.

3.5.1.3 Full cleavage

The peptide was cleaved for 2 h using ~10 mL of 'special reagent K' cleavage cocktail (82.5%/5%/5%/5%/2.5% = TFA/H_2O/Cresol/Thioanisole/1,2-ethanedithiol). TFA was evaporated under a gentile nitrogen stream. Subsequently, the peptide was triturated (2x) using ice cold diethylether, spun down for 5 min at 10000 RPM. The pellet was dissolved in H_2O (10 mL for 41 µmol scale) and lyophilized.

3.5.1.4 Preperative HPLC (Prep-HPLC) – General protocol

For prep-HPLC a BESTA-Technik system attached to a Reprosil Gold 120 C18 column 10 µm (250 x 25 mm) and an ECOM Flash 10 DAD 800 UV detector set on 214 nm was used. The mobile phases used were solvent A (94.9%/5%/0.1% = H_2O/ MeCN /TFA) and solvent B (5%/94.9%/0.1% = H_2O/ MeCN /TFA).

Method: 0% solvent B over 3 min, next 0% to 15% solvent B over 1 min, followed by a linear gradient 15% to 90% solvent B over 86 min and 100% solvent B over 3 min. The obtained fractions where analyzed using a Sciex X500b QTOF LC-MS (see LC-MS high resolution protocol, method B). Pure fractions were combined and stored as lyophilized powders at -20 °C.

3.5.1.5 LC-MS

LC-MS chromatograms and associated mass spectra were acquired using a Shimazu LCMS-2020 system (Method A) or, for high resolution mass spectrometry data, a Sciex X500b QTOF ESI-QToF mass spectrometer couple to a Shimadzu Nexera UHPLC LC40DX3 (Method B). Mobile phases used for LC-MS analysis are solvent A (0.1% formic acid in H_2O) and solvent B (0.1% formic acid in acetonitrile). Solvent C (94.9%/5%/0.1% = H_2O/ MeCN /TFA) was used to dissolve protein mixtures to a concentration of 1 mg/mL.

The following LCMS methods were used:

Method A

Column: Kinetex® 2.6µm XB-C18 100 Å LC Column (50 x 3 mm) UV detector: 214 nM.

LC Method: 0% solvent B over 1 min, followed by a linear gradient 0% to 70% solvent B over 10 min, followed by 70% solvent B over 1.5 min, followed by 70% to 0% solvent B over 4.5 min, flowrate 0.55 mL/min.

Method B (high resolution)

Column: Phenomenex Synergi™ 4 µm Fusion-RP 80 Å LC Column (50 x 2 mm).

LC Method: 0% solvent B over 1 min, followed by a linear gradient 0% to 60% solvent B over 3.5 min, followed by a linear gradient 60% to 95% solvent B over 0.1 min, followed by 95% solvent B over 0.4 min, followed by a linear gradient 95% to 0% solvent B over 0.5 min, followed by 0% solvent B over 1.5 min, flowrate 0.5 mL/min.

MS parameters: General parameters: Method duration: 5 min; Total scan time: 0.276 sec; Estimated cycles: 1086; Intact protein mode: False; Decrease detector voltage: False; Large protein (>70 kDa): False; Ion Source: Source name: TurbolonSpray; Curtain gas: 35 psi; Ion source gas 1: 60 psi; Ion source gas 2: 60 psi; Temperature: 500 ˚C; Experiment: Scan type: TOF MS; Polarity: Positive; Spray voltage: 5500 V; CAD gas: 7; Time bins to sum: 4; Channel 1-4: True; TOF start mass: 350 Da; TOF stop mass 1500 Da; Accumulation time: 0.25; Declustering potential: 80V; Declustering potential spread: 0 V; Collision energy: 10V; Collision energy spread: 0 V; Override Qjet RF value: False.

Method C (high resolution)

When performing the serum stability assay, the following changes were made on the protocol Method B:

LC Method: 0% solvent B over 0.5 min, followed by a linear gradient 0% to 90% solvent B over 5.5 min, followed by 90% solvent B over 2 min, followed by a linear gradient 90% to 0% solvent B over 0.5 min, followed by 0% solvent B over 2 min, flowrate 0.5 mL/min.

3.5.2 Protein synthesis with LCMS spectra

3.5.2.1 MiniMYC with lysine linker 1

Fmoc-Lys(Fmoc)-OH (295 mg, 0.5 mmol, 1 eq.) was dissolved in a HATU solution (0.45M, 0.9 eq.) in DMF (1 mL). Subsequently, DIPEA (200 µL, 2.3 eq.) was added to the amino acid solution. The solution was incubated and shaken for 30 seconds and then added to the Chemmatrix Rink amide resin (50 mg, 41 mmol/g). After 10 min incubation at RT, with occasional shaking, the resin was drained and washed with DMF (3 x 5 mL). Next, the peptidyl resin was washed with 20% piperidine in DMF (5 mL) followed by 5 min incubation of 20% piperidine in DMF (5 mL). The resin was drained by vacuum and washed with DMF (5x 5 mL). The dimeric sequence was completed using the standard SPPS protocol. The final AA was acetylated and cleaved according to the general protocols.

MiniMYC (**1**) was purified using a Biotage® Selekt Flash Purification System coupled to a reverse phase Biotage® Sfär C18 D - Duo 100 Å 30 µm 25g column, further revered to as reversed phase flash chromatograpy (RP-FC). The mobile phase solvents used were: solvent A (H_2O with 0.1% TFA) and solvent B (MeCN with 0.1% TFA). The UV detector was set to 214 nm. The following method was applied to the crude protein mixture:

RP-FC method: 10% solvent B over 1 column volumes (CV), followed by a linear gradient of 10% solvent B to 40% solvent B over 25 CV, followed by a linear gradient of 40% solvent B to 70% solvent B over 2 CV. The fractions were analyzed via LC-MS (Method A). Pure fractions were combined and lyophilized. Yield: 14.7 mg, 2.1 µmol, 16%.

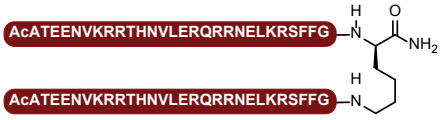

Sequence : $(AcATEENVKRRTHNVLERQRRNELKRSFFG)_2K$

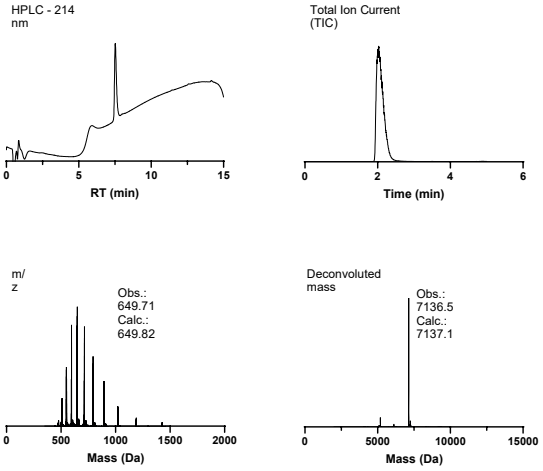

▲LCMS analytics of MiniMYC **1**. The 214 nm LC chromatogram was obtained using LC-MS method A. The TIC, MS and deconvoluted mass chromatograms were obtained using LC-MS method B.

3.5.2.2 MiniMYC monomer 2

MiniMYC monomer **2** was synthesized, acetylated and cleaved according to the general SPPS, acetylation and cleavage protocol, respectively.

MiniMYC monomer **2** was purified using a Biotage® Selekt Flash Purification System with a Biotage® Sfär C18 D - Duo 100 Å 30 µm 25g column. The mobile phase solvents used were: solvent A (H_2O with 0.1% TFA) and solvent B (MeCN with 0.1%TFA). The UV detector was set to 214 nm. The following method was applied to the crude protein mixture:

RP-FC method: 10% solvent B over 1 CV, followed by a linear gradient of 10% solvent B to 50% solvent B over 25 CV, followed by a linear gradient of 50% solvent B to 70% solvent B over 2 CV. The obtained fractions were analyzed according to the LC-MS – low resolution general protocol. Pure fractions were combined and stored as lyophilized powders. Yield: 23.4 mg, 6.7 2.1 µmol , 16%.

Sequence : AcATEENVKRRTHNVLERQRRNELKRSCFA

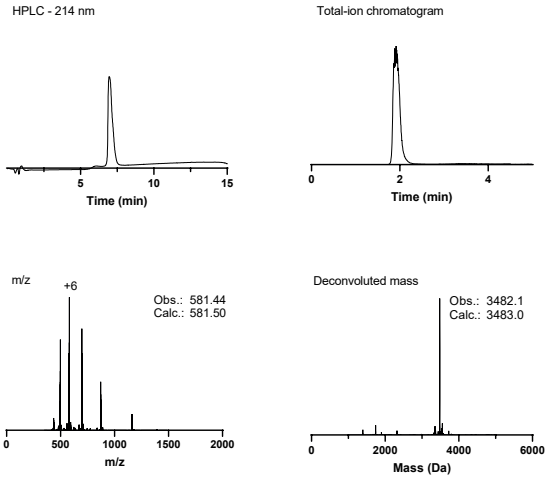

▲LCMS analytics of MiniMYC monomer **2**. The 214 nm LC chromatogram was obtained using LC-MS method A. The TIC, MS and deconvoluted mass chromatograms were obtained using LC-MS method B.

3.5.2.3 MiniMYC with octafluorobiphenyl linker 3

To prepare peptide **3**, stock solutions were prepared in DMF for decafluorbiphenyl (10 mM), DIPEA (80 mM) and TCEP (20 mM). Peptide **2** (11 mg, 3.16 µmol) was dissolved in 314 µL DMF. From each stock solution 314 µL were added to the peptide solution, resulting in the following final concentrations: peptide (3.16 µmol, 2.5 mM, 1 eq.), decafluorbiphenyl (3.16 µmol, 2.5 mM, 1 eq.), DIPEA (25.3 µmol, 20 mM, 8

eq.) and TCEP (6.32 µmol, 5 mM, 2 eq.) in a final volume of 1.26 mL. The solution was shaken for 24 h after which it was quenched by the addition of 1% TFA in H_2O (10 mL) and lyophilized.

MiniMYC dimer (**3**) was purified using a Biotage® Selekt Flash Purification System with a Biotage® Sfär C18 D - Duo 100 Å 30 µm 10 g column. The mobile phase solvents used were: solvent A (H_2O with 0.1% TFA) and solvent B (MeCN with 0.1%TFA). The UV detector was set to 214 nm. The following method was applied to the crude protein mixture:

RP-FC method: 10% solvent B over 1 CV, followed by a linear gradient of 10% solvent B to 50% solvent B over 25 CV, followed by a linear gradient of 50% solvent B to 70% solvent B over 2 CV. The obtained fractions were analyzed according to the LC-MS – low resolution general protocol. Pure fractions were combined and stored as lyophilized powders. Yield 3.5 mg, 482 nmol, 31%.

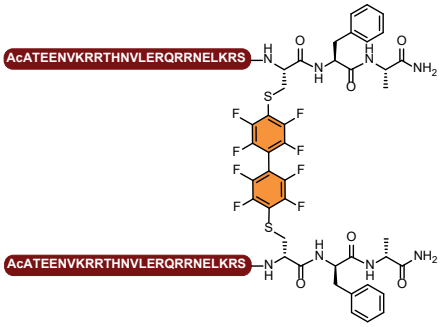

Sequence: $(AcATEENVKRRTHNVLERQRRNELKRSSCFA)_2$-Linker

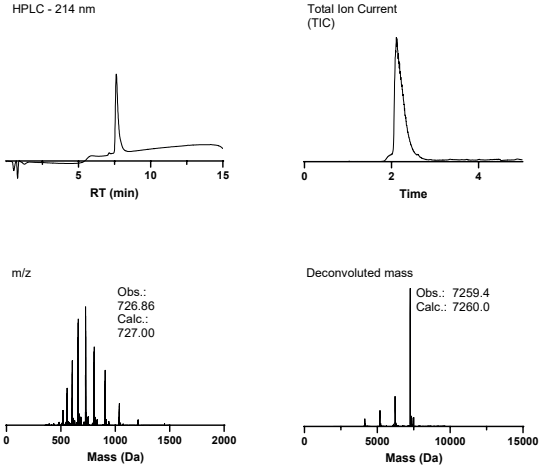

▲LCMS analytics of MiniMYC **3**. The 214 nm LC chromatogram was obtained using LC-MS method A. The TIC, MS and deconvoluted mass chromatograms were obtained using LC-MS method B.

3.5.2.4 MonoMYC 4

MonoMYC **4** was synthesized according to the general SPPS protocol on a 104 µmol scale. Instead of single couplings, double couplings were performed before removal of the Fmoc protection group at each cycle.

MonoMYC **4** was purified twice. The first purification step was performed using a Biotage® Selekt Flash Purification System with a Biotage® Sfär C18 D - Duo 100 Å 30 µm column 25g/50g. The mobile phase solvents used were: solvent A (H_2O with 0.1% TFA) and solvent B (MeCN with 0.1%TFA). Solvent C (94.9%/5%/0.1% = H_2O/MeCN /TFA) was used to dissolve crude protein mixtures. The UV detector was set to 214 nm. The following method was applied to the crude protein mixture:

RP-FC method: 10% solvent B over 2 CV, followed by 20% solvent B over 3 CV, followed by 25% solvent B over 2 CV, followed by 29% solvent B over 3 CV, followed by 32% solvent B over 4 CV, followed by 40% solvent B over 3 CV, followed by 98% solvent B over 5CV. The obtained semipure fractions where analyzed using a Sciex X500b QTOF LC/MS (see LC-MS high resolution protocol). Fractions containing product were combined and lyophilized.

The second purification was performed according to the general prep-HPLC protocol. Yield: 3.6 mg, 516 nmol, 0.5%.

Sequence: AcATEENVKRRTHNVLERQRRNELKRSFFALRDQIPELENNEKAP-KVVILKKATAYILSCA

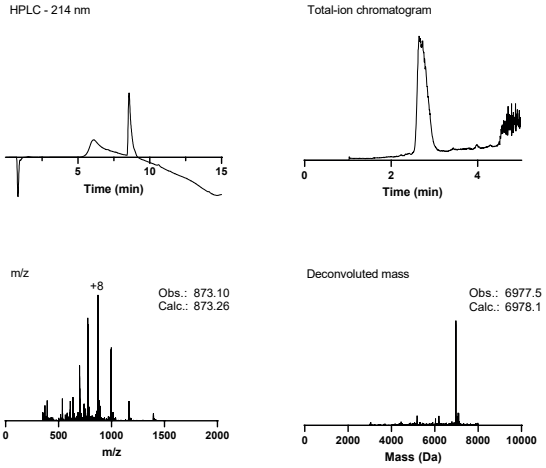

▲LCMS analytics of MonoMYC **4**. The 214 nm LC chromatogram was obtained using LC-MS method A. The TIC, MS and deconvoluted mass chromatograms were obtained using LC-MS method B.

3.5.2.5 DuoMYC with 4,4'-dimethyl-1,1'-biphenyl linker 5

MonoMYC **4** (2.9 mg, 0.34 µmol, 1 eq.) was dissolved in H_2O (338 µL). A stock solution was prepared for 4,4′-Bis(bromomethyl)biphenyl in MeCN (0.4 mM). To the 1 mM MonoMYC **4** solution 2.2 mL NH_4HCO_3 buffer (100 mM, pH = 8) and 0.846 mL of the 4,4′-Bis(bromomethyl)biphenyl stock were added, resulting in a final volume of 3.4 mL and the following concentrations: MonoMYC **4** (0.34 µmol, 0.1 mM, 1 eq.) and 4,4′-Bis(bromomethyl)biphenyl (0.34 µmol, 0.1 mM, 1 eq.). The solution was stirred for 2h and subsequently lyophilized. The crude mixture was either purified according to the prep-HPLC protocol or with RP-FC. For RP-FC the following method was applied to the crude protein mixture:

For RP-FC a Biotage® Selekt Flash Purification System with a Biotage® Sfär C18 D - Duo 100 Å 30 µm column 10g or 50g was used. The mobile phase solvents used were: solvent A (H_2O with 0.1% TFA) and solvent B (MeCN with 0.1%TFA). Solvent C (89.9%/10%/0.1% = H_2O/ MeCN /TFA) was used to dissolve crude protein mixtures. The UV detector was set to 214 nm.

RP-FC method: 0% to 15% solvent B over 0.5 CV, followed by a linear gradient 15% to 56% solvent B over 12.7 CV and 95% solvent B over 2 CV. The obtained fractions where analyzed using a Sciex X500b QTOF LC/MS (see LC-MS high resolution protocol). Fractions containing product were combined and lyophilized. Yield: 1.11 mg, 78.5 nmol, 46%.

Sequence: $(AcATEENVKRRTHNVLERQRRNELKRSFFALRDQIPELENNEKAP-KVVILKKATAYILSCA)_2$-linker

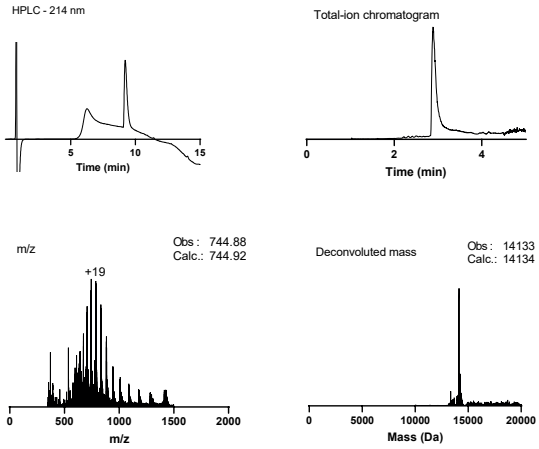

▲LCMS analytics of DuoMYC **5**. The 214 nm LC chromatogram was obtained using LC-MS method A. The TIC, MS and deconvoluted mass chromatograms were obtained using LC-MS method B.

3.5.2.6 MonoMYC 6

MonoMYC **6** was synthesized according to the general SPPS, acetylation and cleavage protocols on a 41 µmol scale. MonoMYC **6** was purified using a Biotage® Selekt Flash Purification System with a Biotage® Sfär C18 D - Duo 100 Å 30 µm column 25g. The mobile phase solvents used were: solvent A (H_2O with 0.1% TFA) and solvent B (MeCN with 0.1% TFA). The UV detector was set to 214 nm. The following method was applied to the crude protein mixture:

RP-FC method: 20% solvent B over 2 CV, followed by a linear gradient of 20% solvent B to 30% for 3 CV, followed by a linear gradient of 30% solvent B to 40% over 22 CV, followed by 100% solvent B over 3 CV. The obtained pure fractions were analyzed using the low resulution LCMS protocol. Fractions containing product were combined and lyophilized. Yield: 17 mg, 2.6 2.1 µmol, 6%.

Sequence: AcVKRRTHNVLERQRRNELKRSFFALRDQIPELENNEKAPKVVILKKATAYILSVA$_\beta$C

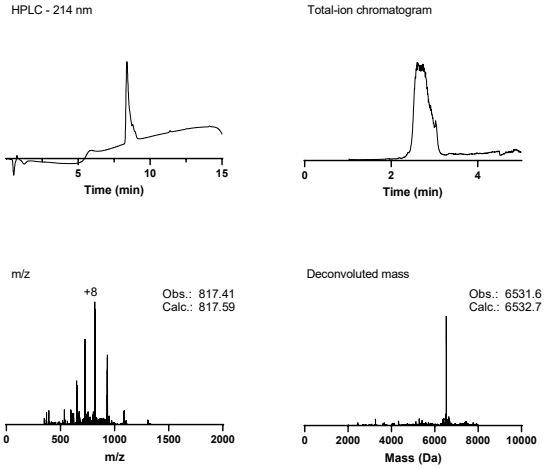

▲LCMS analytics of MonoMYC **6**. The 214nm LC chromatogram was obtained using LC-MS method A. The TIC, MS and deconvoluted mass chromatograms were obtained using LC-MS method B.

3.5.2.7 DuoMYC with octafluorobiphenyl linker 7

MonoMYC **6** (4.24 mg, 0.64 µmol, 1 eq.) was disolved in DMF (58 µL). The following stock solutions were prepared in DMF: DIPEA (0.5M), decalfluorobiphenyl (0.01M) and TCEP (0.1M). To the MonoMYC **6** solution was added from each stock solution: 13 µL of DIPEA (6.4 µmol, 10 eq., 60 mM), 19.5 µL TCEP (1.2 µmol, 0.3 eq., 17.7 mM) and 19.5 µL decafluorbiphenyl (0.19 µmol, 3 eq., 1.77 mM) resulting in a final peptide concentration of 6 mM. The reaction was shaken for 3 days at 37 °C. When precipitation occurred during the reaction, the reaction mixture was sonicated, vortexed and placed back in the shaker. Yield: 1.28 mg, 12%.

DuoMYC **7** was purified using a Biotage® Selekt Flash Purification System with a Biotage® Sfär C18 D - Duo 100 Å 30 µm column 10g. The mobile phase solvents used were: solvent A (H_2O with 0.1% TFA) and solvent B (MeCN with 0.1%TFA). The UV detector was set to 214 nm. The following method was applied to the crude protein mixture:

HPFC method: 20% solvent B over 2 column volumes (CV), followed by a linear gradient of 20% solvent B to 30% for 3 CV, followed by a linear gradient of 30% solvent B to 40% over 22 CV, followed by 100% solvent B over 3 CV. The obtained semipure fractions were analyzed using the low resolution LCMS protocol. Fractions containing product were combined and lyophilized. Yield: 1.28 mg, 95.8 nmol, 12%.

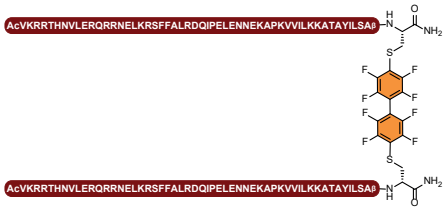

Sequence: (AcVKRRTHNVLERQRRNELKRSFFALRDQIPELENNEKAPKVVILK KATAYILSA$_\beta$C)$_2$-linker

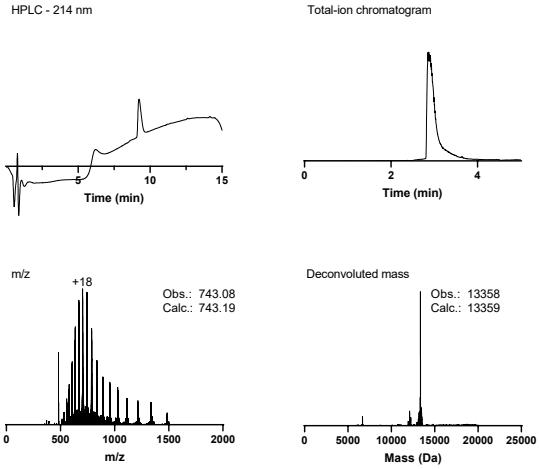

▲LCMS analytics of DuoMYC **7** The 214 nm LC chromatogram was obtained using LC-MS method A. The TIC, MS and deconvoluted mass chromatograms were obtained using LC-MS method B.

3.5.2.8 Unspecifically FITC-labeled DuoMYC 8

DuoMYC **5** (1.55 mg, 0.089 µmol, 1 eq.) was dissolved in 0.1M carbonate buffer (1.55 mL, pH = 9.1), providing a 1 mg/mL solution. FITC in DMSO (51.5 µL of a 1 mg/mL solution, 0.12 µmol, 1.4 eq.) was added to the DuoMYC solution. The mixture was protected from light and reacted for 3.5h. An additional 0.3 eq. of FITC was added and reacted for an additional 3h. Labeled DuoMYC **8** was directly purified using a Biotage® Selekt Flash Purification System with a Biotage® Sfär C18 D - Duo 100 Å 30 µm column 10g. The mobile phase solvents used were: solvent A (H_2O with 0.1% TFA) and solvent B (MeCN with 0.1%TFA). The UV detector was set off. The following method was applied to the crude protein mixture:

RP-FC method: 0% to 15% solvent B over 0.5 CV, followed by a linear gradient 15% to 56% solvent B over 12.7 CV and 95% solvent B over 2 CV. The obtained fractions where analyzed using a Sciex X500b QTOF LC/MS (see LC-MS high resolution protocol). Fractions containing product were combined and lyophilized yielding FITC-labelled DuoMYC (1.29 mg, 71.55 nmol, 80%) containing 1, 2 and 3 molecules

of fluorescein. For stock preparations an average molecular weight of 18027.37 g/mol was used.

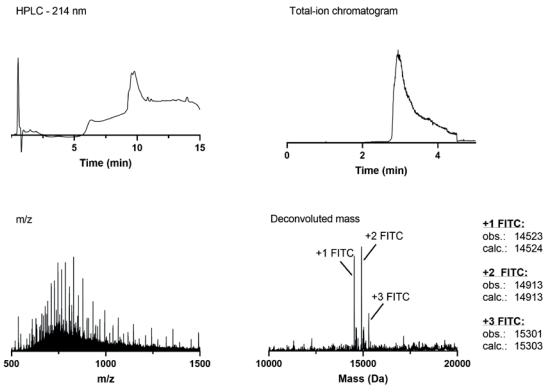

▲LCMS analytics of DuoMYC **8** The 214 nm LC chromatogram was obtained using LC-MS method A. The TIC, MS and deconvoluted mass chromatograms were obtained using LC-MS method B.

3

3.5.2.9 Unspecifically FITC-labeled Omomyc 9

Omomyc expressed in E.Coli and purified (see 4.2, 4.4 mg, 287 nmol, 1 eq.) was dissolved in 440 µL 0.1M carbonate buffer pH 9.1 to a concentration of 1mg/mL. Subsequently, a 2.6mM solution of FITC in dmso (22 µL, 402 nmol, 1.4 eq.) was added and the solution was stirred at rt and protected from light for 4h. The crude product was then purified by reverse phase column using a Biotage® Selekt Flash Purification System with a Biotage® Sfär C18 D - Duo 100 Å 30 µm column 10g. The mobile phase solvents used were: solvent A (H_2O with 0.1% TFA) and solvent B (MeCN with 0.1%TFA). After column chromatography the product was further purified by spinning through an Advance spin column with a molecular weight cutoff 3 kD to remove residual FITC. This procedure was repeated three times followed by lyophilization yielding FITC-labelled Omomyc (0.87 mg, 58 nmol, 12%) containing 1, 2, 3, and 4 molecules of fluorescein. For stock preparations an average molecular weight of 12500.75 g/mol was used.

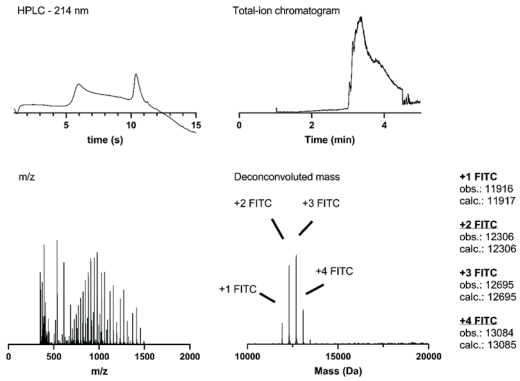

▲LCMS analytics of Omomyc **9** The 214 nm LC chromatogram was obtained using LC-MS method A. The TIC, MS and deconvoluted mass chromatograms were obtained using LC-MS method B.

3.5.3 Biochemistry

3.5.3.1 Overview of buffers used

Bacterial cell lysis buffer	20mM Tris-HCl, pH 8, 0.5 M NaCl, 3mM $MgCl_2$, 0.05% DNAse,complete EDTA free protease inhibitor (1 tablet freshly added in 50 mL buffer)
EK cleavage buffer	200 mM Tris-HCl, pH 7.4, 0.5 M NaCl, 20 mM $CaCl_2$
EK dilution buffer	20 mM Tris-HCl, pH 7.4, 200 mM NaCl, 2 mM $CaCl_2$, 50% glycerol
Affinity wash buffer	20 mM Tris-HCl, pH 8, 0.5 M NaCl, 10mM imidazole
Affinity elution buffer	20 mM Tris-HCl, pH 8, 0.5 M NaCl, 500mM imidazole
EMSA binding buffer	20 mM HEPES, pH 8.0, 150 mM NaCl, 5% glycerol, 1 mM EDTA, 2 mM $MgCl_2$, 0.5 mg/mL of BSA, 1 mM DTT and 0.05% NP-40
EMSA running buffer	0.5x TBE, 50 mM Tris borate, pH 8.3, 1 mM EDTA

3.5.3.2 Expression of Omomyc in E.Coli

Plasmid pET-30 with Omomyc was gratefully received from the research group of Prof. Dr. Eilers at University of Wuerzburg (see annex for plasmid sequence) and sequenced before use.

Plasmids were transformed into competent ArcticXpress DE3 RIL cells (Agilent) by heat shock. 2 µL of 10% β-mercaptoethanol were mixed with 100 µL of competent cell suspension thawed on ice and incubated for 10 minutes on ice. Next, 25 ng of plasmid DNA were added and the cells incubated for another 30 minutes on ice. The cells were then heat-shocked in a water bath for 20 seconds at 42 °C and subsequently incubated on ice for 2 minutes followed by the addition of 0.9 mL SOC media and incubation at 37 °C, 250 rpm for 1 h. Cells were pelleted by centrifugation, 0.9 mL of the supernatant decanted and the pellet resuspended in the remaining 100 µL of media. Subsequently, cells were plated for selection on LB agar with kanamycin and gentamicin and incubated at 37 °C overnight.

Single colonies were picked from the plate and cultured overnight at 37 °C and 200 rpm in 100 mL of LB media containing kanamycin and gentamicin. Next, 3x2 L of LB media containing kanamycin and gentamicin in 5 L Erlenmeyer flasks were inoculated with 25 mL of preculture and grown at 37 °C, 200 rpm until an OD of 0.8 was reached. The temperature was then set to 14 °C and protein expression induced by addition of 100 µM of IPTG. Protein expression was conducted overnight for 18 h after which the cells were harvested by centrifugation (5,000g, 4 °C, 12 min.), the pellet resuspended in lysis buffer (20mM Tris-HCl, pH 8, 0.5 M NaCl, 3mM $MgCl_2$, 0.05% DNAse,complete EDTA free protease inhibitor) and the cells lysed by pressure lysis. Cell debris was removed by ultracentrifugation (35,000 rpm, 4°C, 45 min.).

3.6.3.3 Purification of his-tagged proteins

The supernatant after ultracentrifugation was purified using an ÄKTA start protein purification system equipped with a 5 mL HisTrap HP His tag protein purification column (Cytiva). After washing out unbound protein with wash buffer (20 mM Tris-HCl pH 8, 0.5 M NaCl, 10 mM imidazole) the protein was eluted using a gradient of 10 mM to 500 mM imidazole in the same buffer over 40-50 column volumes. Fractions with protein were analyzed for protein content and purity by SDS-PAGE.

3.5.3.4 General protocol for SDS-PAGE

Samples were mixed with the appropriate amount of 4x LB buffer containing β-mercaptoethanol and heated to 95 °C for 5 minutes to denature proteins. Samples were then loaded onto acrylamide gels of the desired percentage (made using acrylamide 37.5:1 acrylamide/Bis) and ran at room temperature at 150V for one hour. If desired, gels were stained for at least 20 minutes with coomassie blue staining solution followed by at least three rounds of destaining with destaining solution (50% MeOH, 40 % H_2O, 10% AcOH). Stained gels were scanned on a Bio-Rad ChemiDoc MP machine.

3.5.3.5 General protocol for buffer exchange

The combined fractions obtained from Ni-column purification were incubated with TCEP (500 µM-1mM) to break any possible formed disulfide bonds. The buffer was then exchanged by subjecting the protein to column chromatography on a Biotage® Selekt Flash Purification System equipped with a Biotage® Sfär C18 D - Duo 25g or 50g column and a stepwise gradient of 0 % MeCN in water, 50 to 100% MeCN water). The combined fractions containing the protein were lyophilized, yielding the His-tagged or final protein as TFA salt.

3.5.3.6 His-tag cleavage by enterokinase

Omomyc was dissolved at 2 mg/mL in EK cleavage buffer (200 mM Tris-HCl, pH 7.4, 0.5 M NaCl, 20 mM $CaCl_2$) and after addition of 10 u/mL enterokinase (previously diluted in dilution buffer, 20 mM Tris-HCl, pH 7.4, 200 mM NaCl, 2 mM $CaCl_2$, 50% glycerol), the protein was incubated overnight. Cleaved Omomyc was purified purified using an ÄKTA start protein purification system equipped with a 5 mL HisTrap HP His tag protein purification column with the protein being eluted in the flowthrough. Fractions were checked fro protein content and purity using SDS-PAGE and the buffer was exchanged using the general protol for buffer exchange.

3.5.3.7 Electromobility shift assay (EMSA)

For EMSAs, 14 µL (15 µL for no protein control) water were mixed with 1 µL of 20x FAM-labelled dsDNA construct (IRD700-ACC CCA C**CA CGT G**GT GCC T, one one strand labelled, (Integrated DNA technologies, Leuven, Belgium), 1 µL of 20x protein in water and 4 µL of 5x EMSA buffer (final buffer concentration: 20 mM HEPES, pH 8.0, 150 mM NaCl, 5% glycerol, 1 mM EDTA, 2 mM $MgCl_2$, 0.5 mg/mL of BSA, 1 mM DTT and 0.05% NP-40). The samples were incubated for 30 minutes at room temperature, placed on ice and incubated for another 15 minutes after which 15 µL of the samples were loaded onto a 10% acrylamide TBE gel which was pre run before for 1h at 75V at 4 °C in 0.5x TBE. Samples were run for 20 minutes at 120 V followed by 40 minutes at 100 V at 4 °C in 0.5x TBE and subsequently scanned on on a Bio-Rad ChemiDoc MP machine.

3.5.3.8 Cell culture

Cells were cultured at 37°C in 5% CO_2 atmosphere. Cell lines were cultured in ATCC recommended media and split twice a week before confluency was reached.

3.5.3.9 Reporter gene assay

3.5.3.9.1 Reporter gene assay in HEK293T cells

The reporter gene assay was performed using Cignal reporter assay (CCS-012L, Qiagen) according to the manufacturer's protocol with slightly prolonged incubation times. In brief, HEK293T cells were harvested and resuspended in OptiMEM media containing 5% FBS and 1% non essential amino acids. 40,000 cells were seeded per well in a 96-well plate and transfection cocktail of either cignal reporter or positive or negative control reporter along with attractene transfection reagent was added and the cells incubated overnight. Next, media was changed to assay media (OptiMEM, 0.5% FBS, 1% NEAA, Pen/Strep) and the cells were incubated for 8 hours after which the media was replaced by 75 µL assay media containing the different proteins/

control compounds at the required concentration and the cells were incubated for 16-24 hours. Luciferase assay was then performed using a luciferase assay kit (E2940, Promega). Cells were lysed by addition of 75 µL of DualGlo Luciferase assay reagent and incubated for 15 minutes after which Luciferase luminescence was measured in on a Bio-Rad ChemiDoc MP machine. Subsequently, 75 µL of DualGlo Stop & Glo reagent were added and the Renilla luciferase luminescence measured after 15 minutes of incubation time. Signal was normalized against cell number by calculating the ratio of firefly and renilla luminescence and eventually these signals were normalized against the untreated control. All experiments were done at least in technical duplicates.

3.5.3.9.2 Reporter gene assay in Hela cells

When performing the assay using Hela cells, the following changes were made to the protocol described in 4.9.1: 20,000 Hela cells were seeded per well and double the amount of DNA was used.

3.5.3.10 Serum stability assay

A 10% Human serum solution was prepared in DPBS (pH = 7.3). From the peptide stock (1 mM in H_2O) peptide was diluted to a final concentration of 60 µM in the 10% serum solution. The mixture was vortexed immediately after protein addition and 5 µL aliquotes were mixed with 5 µL of a 20% TFA solution in H_2O (T = 0) to quench the human serum, resulting in protein precipitating. Subsequently, the peptide serum solution was incubated at 37 ˚C using a BIO-RAD T100™ Thermal Cycler with the lid set on 95 °C. At indicated timepoints 5 µL aliquotes were mixed with 5 µL of 20% TFA in H_2O, respectively. The pellet was diluted 5.5x with addional DPBS to redissolve the precipitated protein pellet. This solution was analyzed according to the high resolution LCMS protocol (Method C). As internal standard (IS), the extracted-ion chromatogram (XIC) from 1233.5184 was used belonging to human serum albumin. After measurement, the XIC belonging to the protein, +8 peak for MonoMYC **4**, +19 peak for DuoMYC **5** and +13 peak for Omomyc, and IS were extracted from the total-ion chromatogram (TIC). Using Graphpad Prism 9, the area under the curve (AUC) from each timepoint was calculated, normalized against the AUC of IS followed by normalization against T = 0 and plotted. Next, a nonlinear regression – One phase decay analysis was performed to obtain $t_{1/2}$ with a plateau constant equal to 0 and Y_0 set to 1. The assay was performed in independent triplicates.

3.5.3.11 Circular Dichroism (CD)

All lyophilized proteins were dissolved in H_2O to a concentration of 1 mM. For CD measurements these proteins were diluted to 10 µM (MiniMYC **1**, MiniMYC **3**,

DuoMYC **5**) or 20 µM (MonoMYC **4**, MonoMYC **6**, DuoMYC **7**) in a 20 mM K_2HPO_4 solution (pH = 7.4) with a final volume of 200 µL. CD samples were measured at 37 °C using a Jasco J-815 CD spectrometer with a 1 mm path length quartz cuvette. The following parameters were used for a full wavelength scan: wavelength = 260-190 nm; Data pitch = 1 nm; scanning mode = continuous; scanning speed = 100 nm/min; response = 1, BW = 1, accumulation = 3. For analysis, all curves were smoothened using Graphpad Prism 9 by averaging 10 neighboring datapoints and a 4th order smoothing polynomial. All curves were normalized against their concentration (10 µM/20 µM), pathlength (0.1 mm) and peptide bonds (n) using the following formula:

$$\left[\emptyset\right] = \frac{100*\emptyset_{obs}}{c*n*l}$$

With θ in deg*cm^{2}*dmol^{-1}, θ_{obs} in mdeg, concentration (c) in mM, peptide bonds (n) and path length of cuvette in cm. The graph was plotted using GraphPad Prism 10.1.0.

3.5.3.12 Biolayer interferometry (BLI)

DuoMYC **5** or **7** was diluted in H_2O to a concentration of 120 µM and diluted further in kinetic buffer (1x PBS, BSA 0.1%, Tween-20 0.02%) with a final volume of 200 µL. The following 5' biotinylated hairpin sequence was used: TT CCT **CAC GTG** GCA TTT GGG TGC **CAC GTG** AGG (Integrated DNA technologies, Leuven, Belgium). A 10 µM DNA stock in H_2O was incubated at 95 °C for 5 minutes, cooled down to RT and diluted to 1 µM in kinetic buffer, which could be loaded on the Sartorius Octet R4. Each experiment was performed in a 96-well plate. Before each measurement, the sensortips were incubated in 200 µL kinetic buffer for at least 10 minutes. All concentration curves were measured at 25 °C while shaking. During each experiment to following steps were performed: the sensortips were incubated for 1 minute in kinetic buffer, followed by a 1 minute DNA loading step, followed by 1 minute of incubation in kinetic buffer, followed by 10 minute sample incubation (association), followed by 10 minutes kinetic buffer incubation (dissociation). The same experiment was repeated without loading DNA on the sensortips to obtain the background signal that could be removed from the obtained BLI spectra. The experiment was performed in independent triplicates from which the average K_D was calculated.

3.5.3.13 Fluorescence microscopy

Hela cells were harvested and seeded at a density of 10,000 cells/well in a 96-well plate. In case of 24h compound treatment the cells were let to attach to the well for 6h and then treated with 75µL of the compounds at the desired concentration in MEM media for 24h. The media was then aspirated and the cells treated with 0.2µg/mL Hoechst nuclear stain for 30 minutes. In case of 4h compound treatment, the cells were let to attach to the wells overnight followed by treatment with 75 µL of the

compounds at the desired concentraton along with 0.2 µg/mL Hoechst nuclear stain in MEM for 4h. For both treatment times cells were then washed 2x with fresh MEM and the live cells immediately imaged on a Nikon Ti2 microscope equipped with a plan apo 40x/0.95 air objective using a 405nm laser for Hoechst and a 488nm laser for fluorescein excitation.

3.5.3.14 RNA sequencing

HCT116 cells were harvested and seeded at a density of 200,000 cells/well in 12-well plates. Cells were then grown overnight and subsequently treated for 24h with 5 µM DuoMyc, 10 µM Omomyc or vehicle in McCoy5a media supplemented with 10% FBS, 1% Pen/Strep and Glutamax. Total RNA was isolated using Qiagen RNeasy Plus Mini Kit (74134) and dissolved in RNAse free water. Samples were shipped to and sequencing was performed by Novogene GmbH (Planegg, Germany). Quality of the raw .fastq files was checked with FastQC v0.12.1. The BBTools software v3.62 (bbduk command) was used to trim adapter sequences and 3' quality decrease, remove PhiX contaminant reads and filter out low quality reads. Filtered reads were aligned to the human genome (Ensembl release 112, Homo_sapiens.GRCh38.112) with STAR v2.7.10b in -quantMode GeneCounts mode to quantify gene-level counts. Differential gene expression analysis between DuoMYC **5** or Omomyc treatment and untreated control was performed in python using the PyDESeq2 v0.4.10 package. Differentially expressed genes were selected based on shrunk Log2 fold change > 0.5 or < -0.5 and adjusted p-value < 0.05. Pre-ranked Gene Set Enrichment Analysis (GSEA) was performed with the gseapy v1.1.3 package with the Hallmark gene sets from the Molecular Signatures Database (MsigDB).

3.5.4 Molecular Dynamic simulations

The pdb structure of Omomyc bound to DNA was retrieved from the PDB (id=5I50) and subsequently prepared for MD using Maestro's 2022-3 protein preparation wizard. Thereafter, a system was build using the desmond system builder, MD simulations were performed using the OPLS4 forcefield under the NPgT ensemble at a temperature of 300K using 2fs timesteps. Simulations were performed in triplicate using a different random seed for the initial velocities, and the resulting 500ns trajectories were subsequently analyzed using the desmond simulation event analysis. All structural images were generated using PyMOL.

3.6 Supplementary Figures and Tables

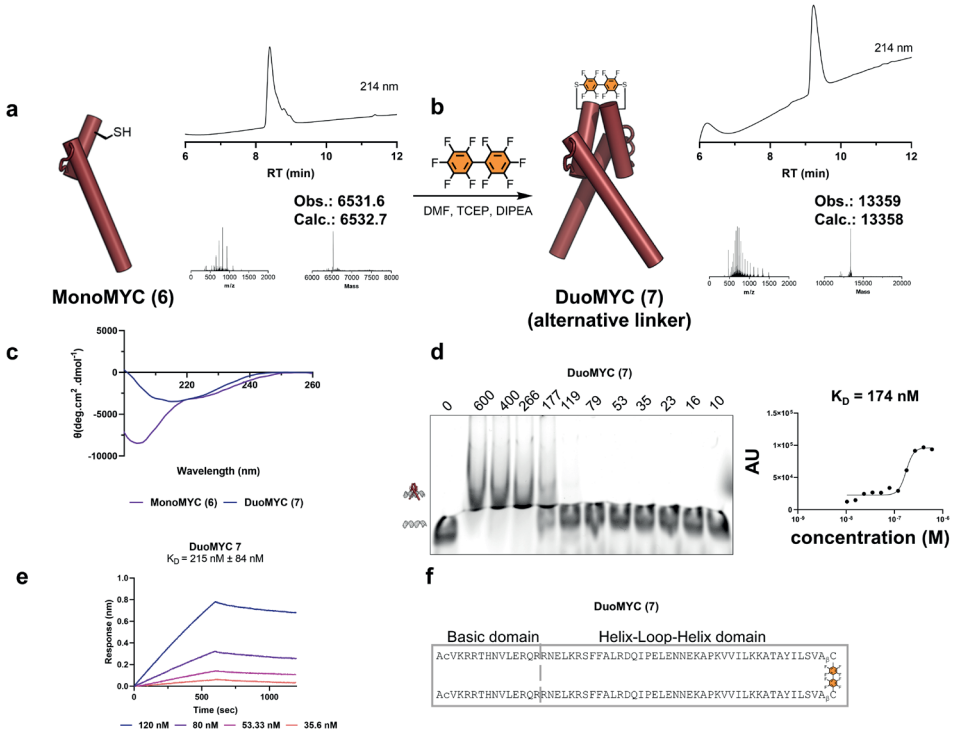

▲Figure S3.1. DuoMYC 7 with alternative (octafluorophenyl) linker binds E-Box with nanomolar affinity. (a) SPPS of monomeric variant **6** with LCMS analysis. b) Dimerization of **6** with decafluorobiphenyl, leading to DuoMYC **7**. c) DuoMYC **7** displays the CD spectrum of a partial α-helix while MonoMYC **6** exhibits the one of a random coil with partial helical structure when measured in absence of DNA. d) DuoMYC **7** binds to E-Box with a K_D = 174 nM. e) Binding evaluation by biolayer interferometry shows a KD of 215 nM for DuoMYC **7**. f) Sequence of DuoMYC **7**. General SPPS coupling conditions: peptidyl resin incubated with Fmoc-AA-OH (10 eq.), HATU (9 eq.) and DIPEA (29 eq.) in DMF for 8 minutes at 70 °C. Fmoc was removed with 20% piperidine + 2% formic acid in DMF (4 minutes at 70 °C). General CD protocol: Protein 10/20 µM in 20 mM K_2HPO_4 solution (pH = 7.4) was measured at 37 °C between 190 nm and 260 nm. General EMSA protocol: Fluorescently-labelled dsDNA construct (IRD700-ACCCCACCACGTGGTGCCT, final concentration 4 nM) was preincubated with protein in EMSA buffer (20 mM HEPES, pH 8.0, 150 mM NaCl, 5% glycerol, 1 mM EDTA, 2 mM). General BLI protocol: Protein was dissolved in kinetic buffer (1x PBS, BSA 0.1%, Tween-20 0.02%) with a final volume of 200 µL and measured against a 5' biotinylated hairpin with the sequence: TT CCT **CAC GTG** GCA TTT GGG TGC **CAC GTG** AGG.

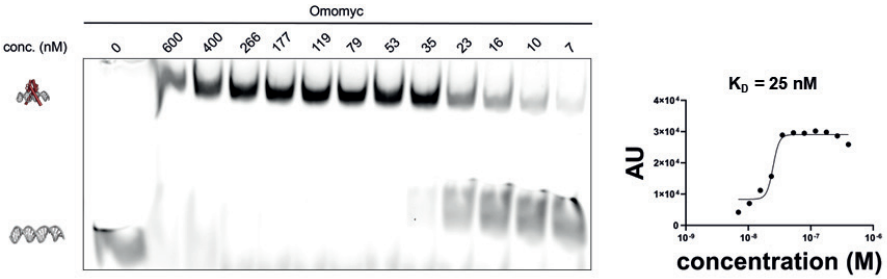

▲Figure S3.2 Omomyc binds to E-box DNA with an affinity of 25 nM. General EMSA protocol: Fluorescently-labelled dsDNA construct (IRD700-ACCCCACCACGTGGTGCCT, final concentration 4 nM) was preincubated with protein in EMSA buffer (20 mM HEPES, pH 8.0, 150 mM NaCl, 5% glycerol, 1 mM EDTA, 2 mM)

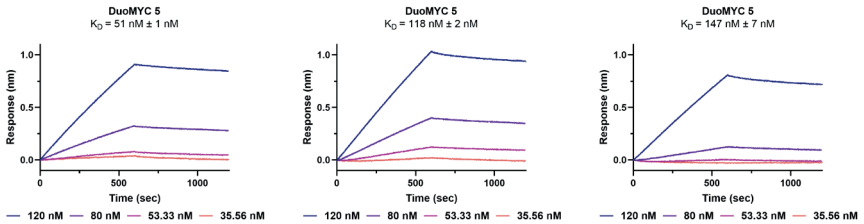

▲Figure S3.3 Three independant experiments to determine the K_D of DuoMyc 5 in a BLI assay. K_D (1) = 51 nM, K_D (2) = 118 nM, K_D (3) = 147 nM. General BLI protocol: Protein was dissolved in kinetic buffer (1x PBS, BSA 0.1%, Tween-20 0.02%) with a final volume of 200 µL and measured against a 5' biotinylated hairpin with the sequence: TT CCT **CAC GTG** GCA TTT GGG TGC **CAC GTG** AGG.

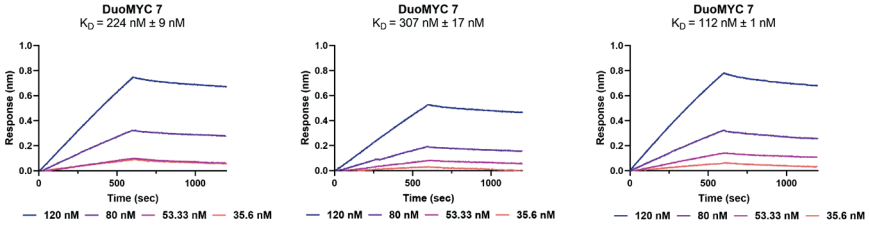

▲Figure S3.4 Three independant experiments to determine the K_D of DuoMyc 7 in a BLI assay. K_D (1) = 224 nM, K_D (2) = 307 nM, K_D (3) = 112 nM. General BLI protocol: Protein was dissolved in kinetic buffer (1x PBS, BSA 0.1%, Tween-20 0.02%) with a final volume of 200 µL and measured against a 5' biotinylated hairpin with the sequence: TT CCT **CAC GTG** GCA TTT GGG TGC **CAC GTG** AGG.

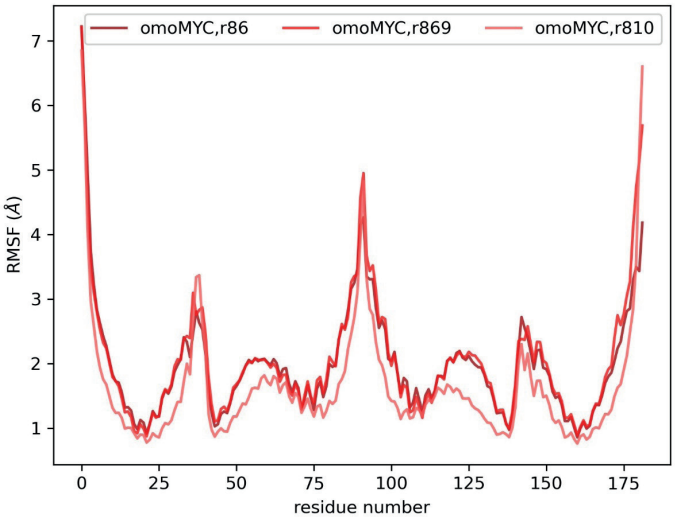

▲**Figure S3.5**. RSMF plot of Omomyc (500 ns MD simulation).

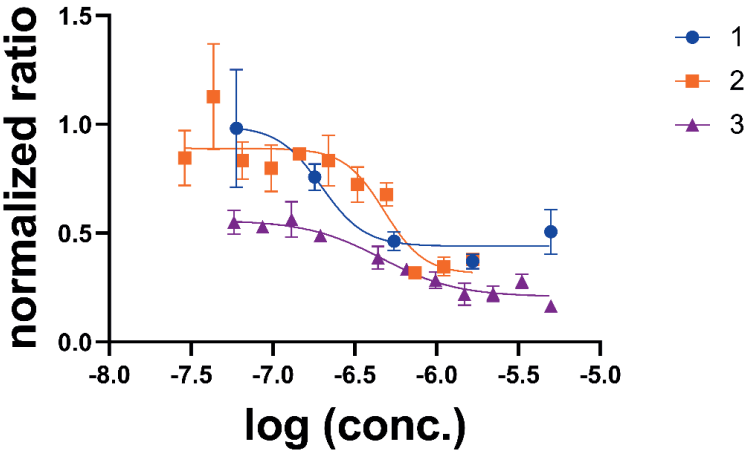

▲**Figure S3.6. Three independant experiments to determine the EC_{50} of DuoMyc 5 in a reporter gene assay.** Curves were fitted to logarithmized data and results indicate EC_{50}s in the nanomolar range. EC_{50}(1) = 198 nM, EC_{50}(2) = 480 nM, EC_{50}(3) = 464 nM.

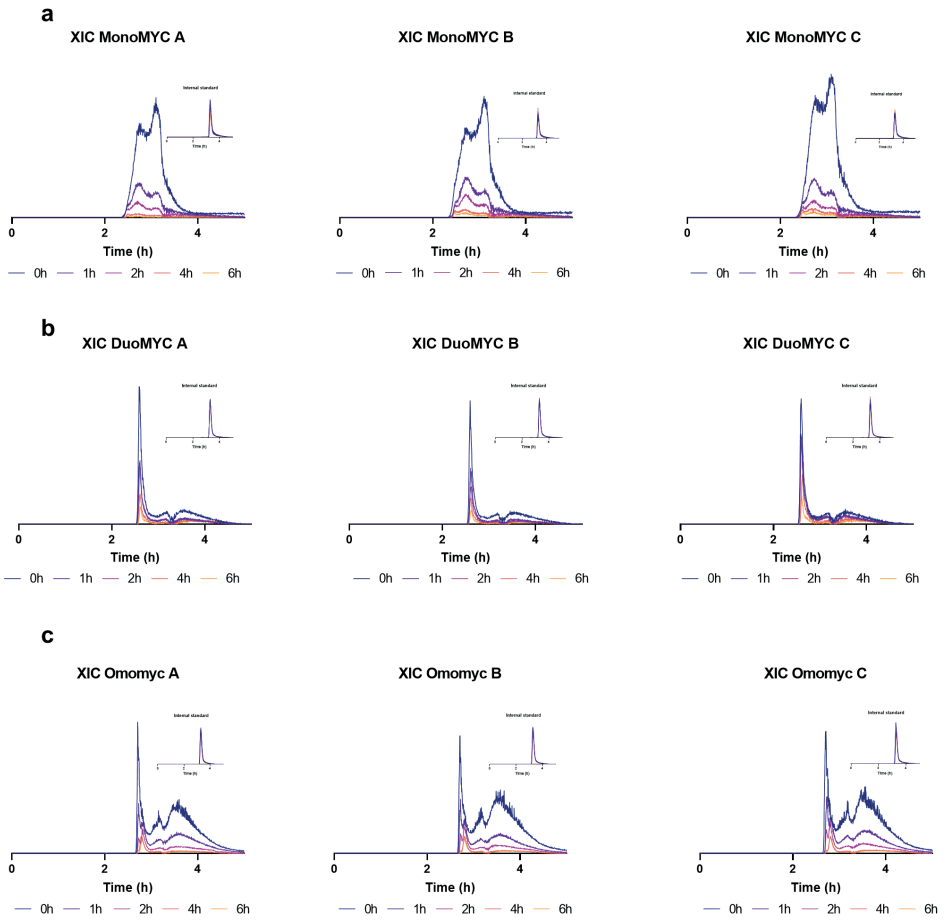

▲**Figure S3.7**. Extracted Ion currents with their corresponding IS from three independant experiments to determine the $t_{0.5}$ of a) MonoMYC **4** b) DuoMyc **5** and c) Omomyc in a serum stability assay.

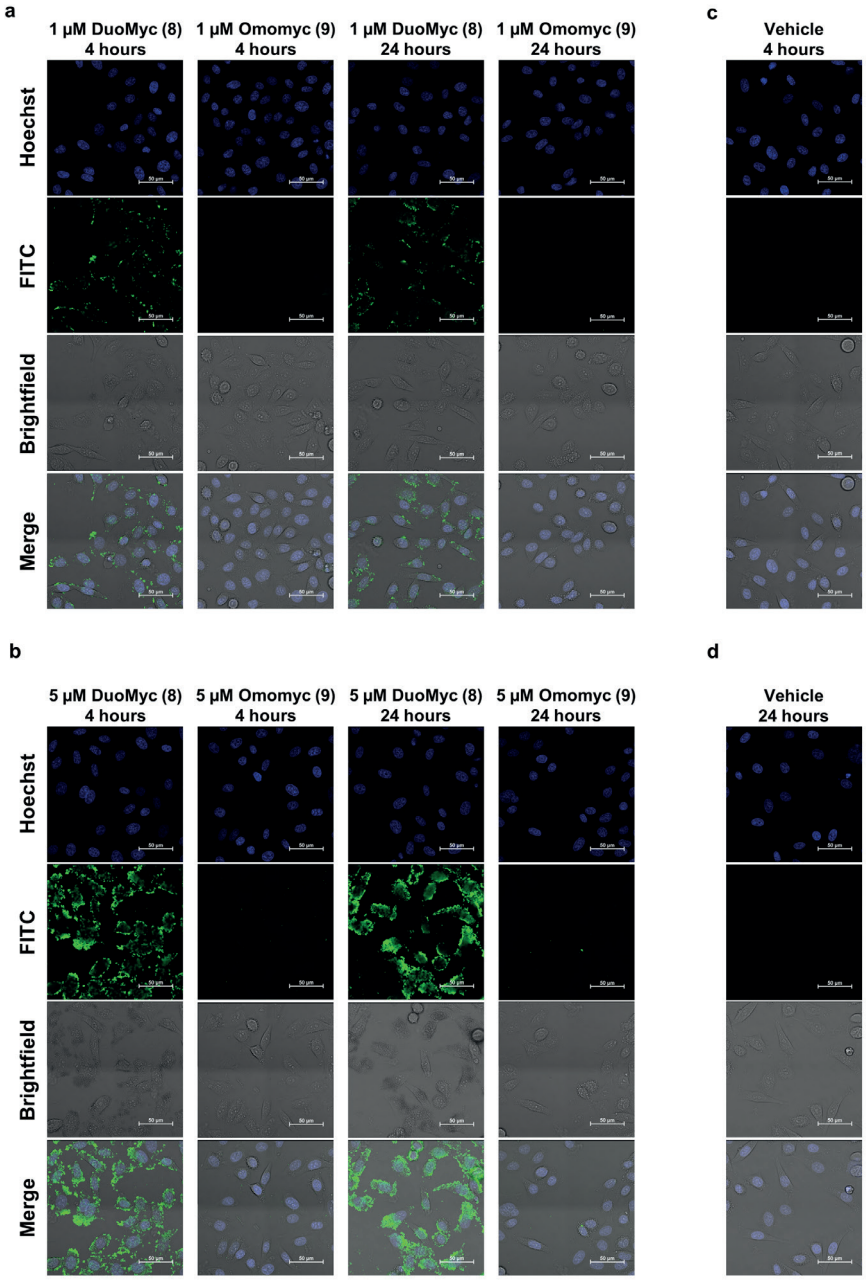

▲Figure S3.8. Confocal fluorescence microscopy images of Hela cells treated with DuoMYC 8, fluorescein-conjugated Omomyc or vehicle at the indicated concentration for different times. (a) A second set of images of Hela cells treated with proteins at 1 µM concentration. (b) Hela cells treated with proteins at 5 µM concentration. (c,d) Cells treated with vehicle for 4 h (c) and 24 h (d). Images shown were stitched from four acquired images.

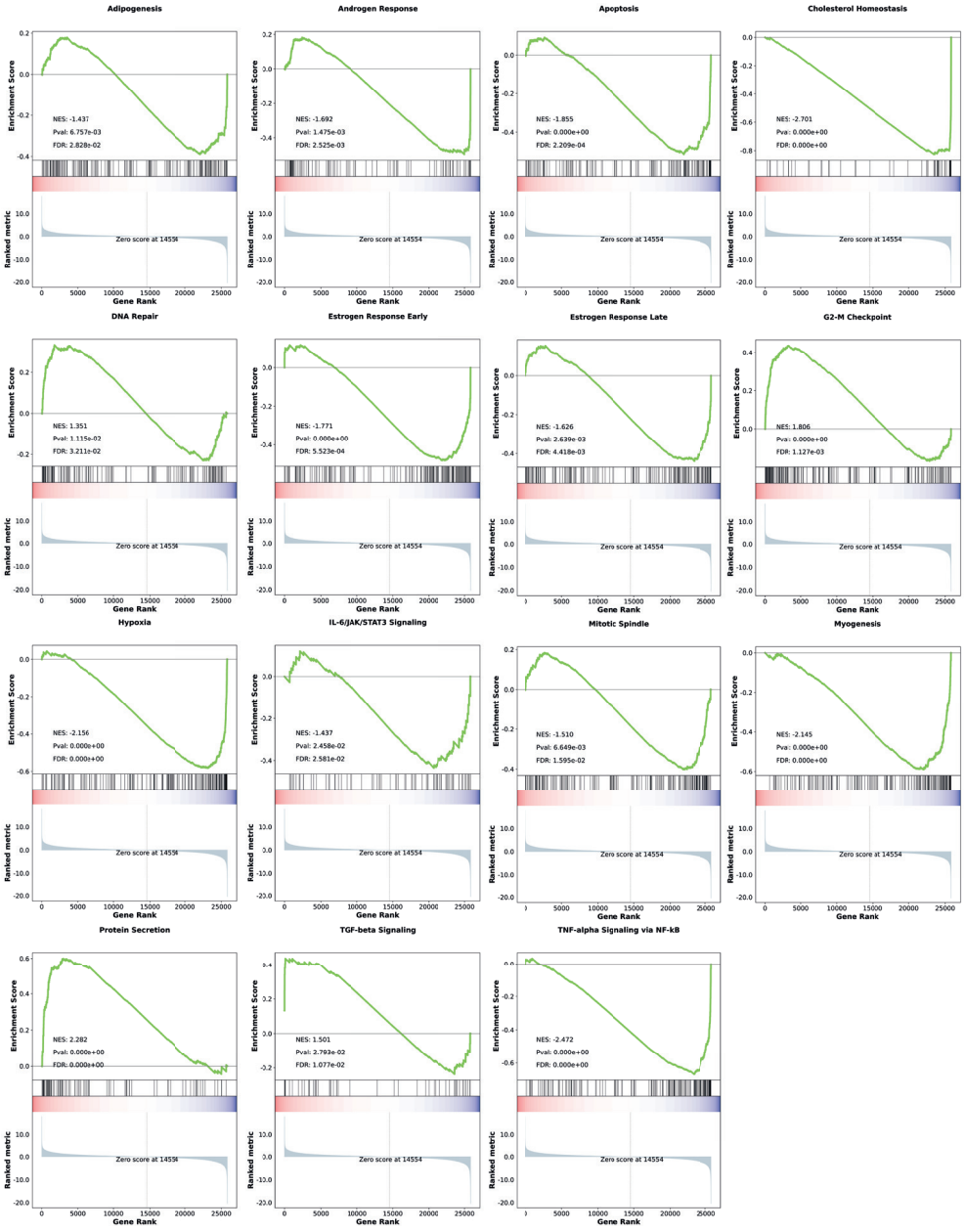

▲**Figure S3.9.** GSEA plots of differently expressed pathways by DuoMyc **5**.

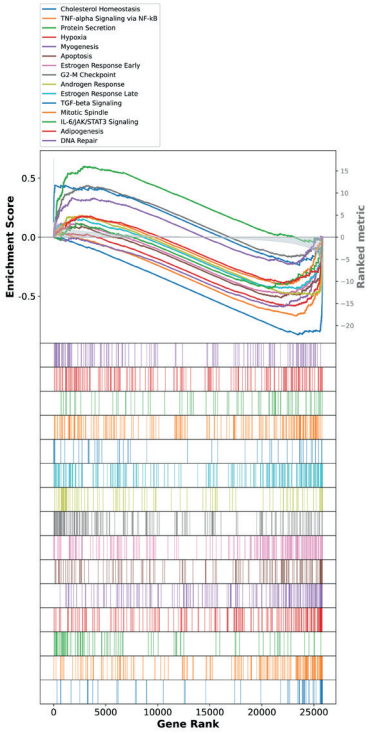

▲**Figure S3.10.** All GSEA plots of differently expressed pathways by DuoMYC **5** combined.

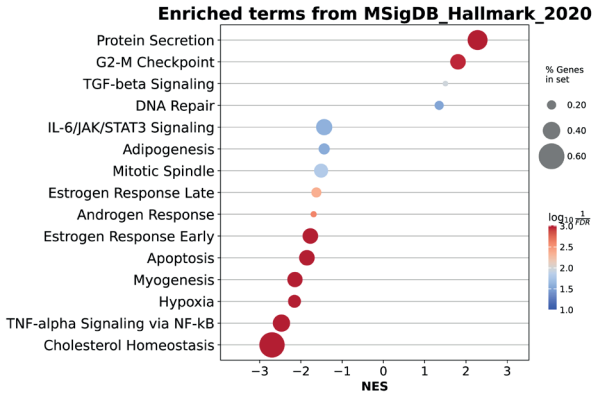

▲**Figure S3.11**. GSEA dotplot of differently expressed pathways by DuoMYC **5**

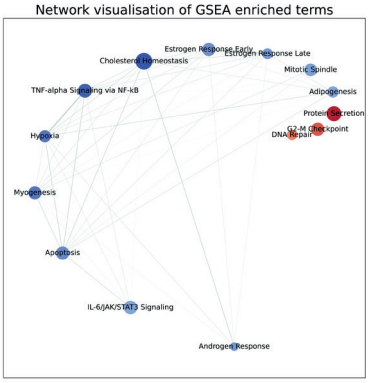

▲**Figure S3.12.** Network visualisation of GSEA enriched terms by DuoMYC **5**

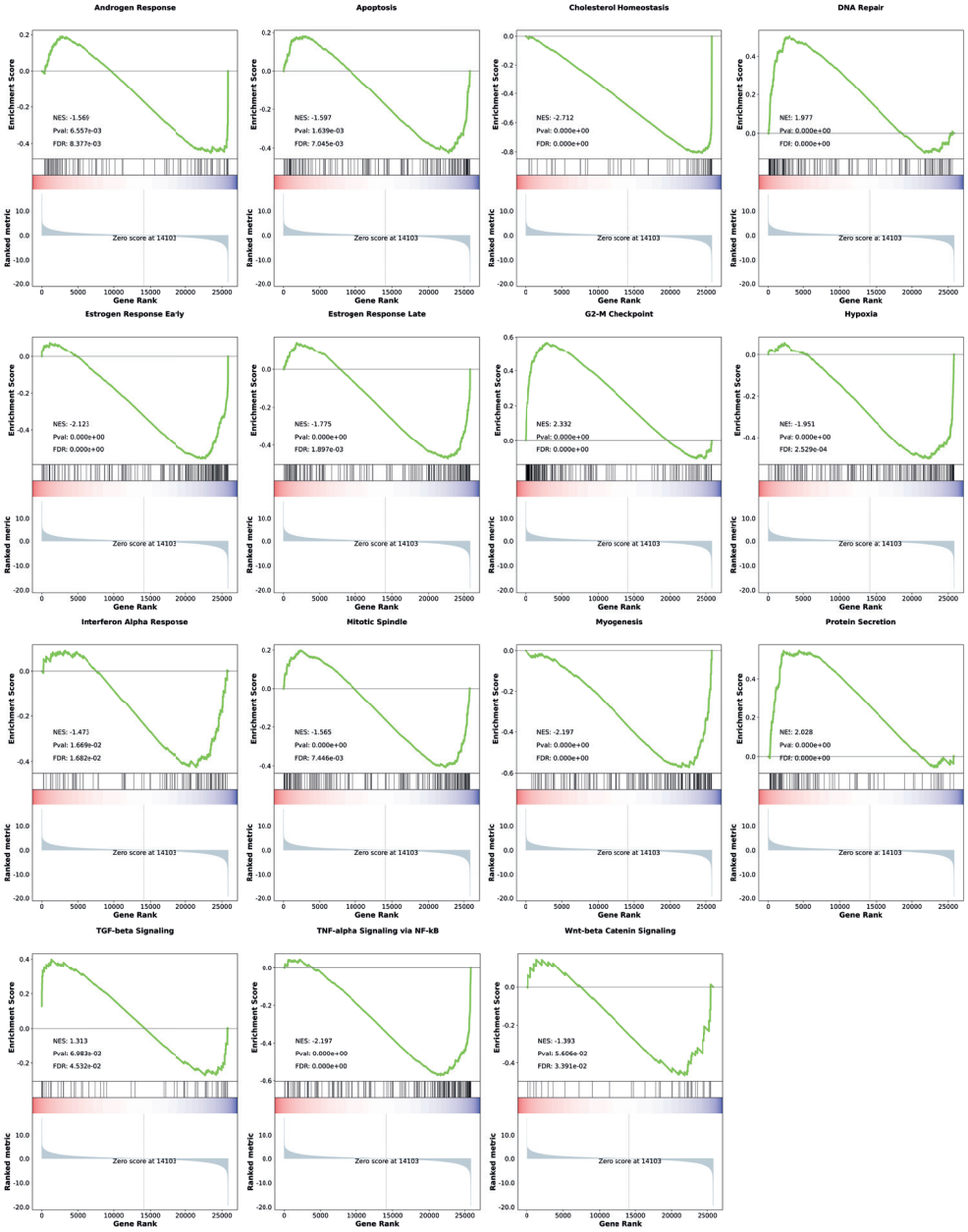

▲**Figure S3.13.** GSEA plots of differently expressed pathways by Omomyc.

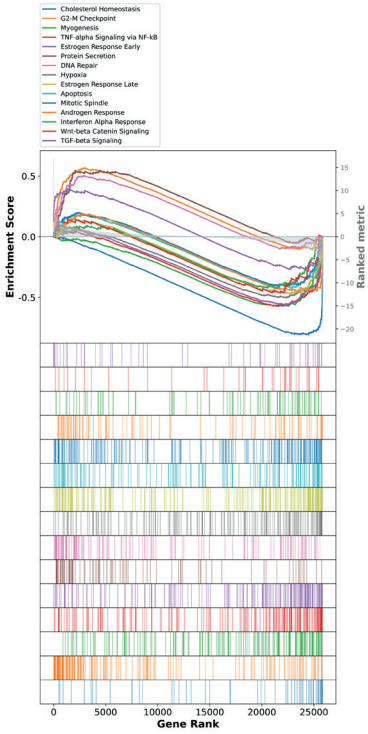

▲**Figure S3.14.** All GSEA plots of differently expressed pathways by Omomyc combined.

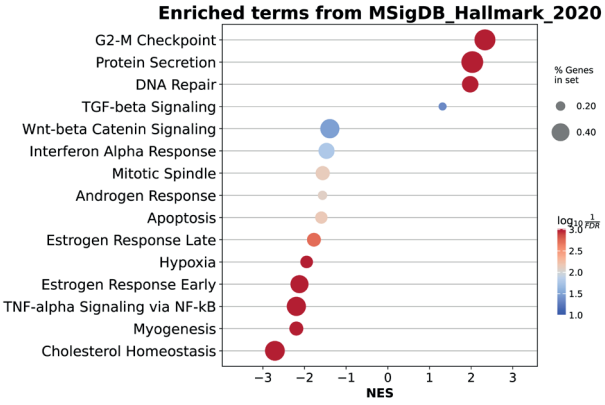

▲**Figure S3.15**. GSEA dotplot of differently expressed pathways by Omomyc.

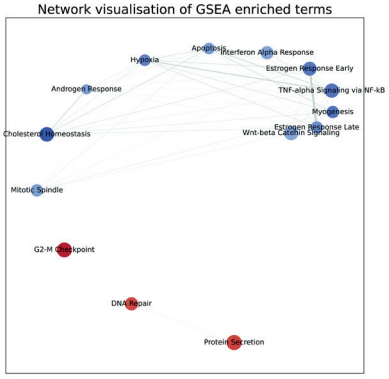

▲**Figure S3.16.** Network visualisation of GSEA enriched terms by Omomyc.

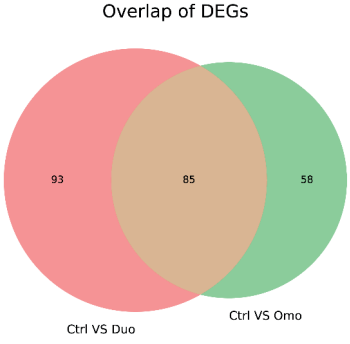

▲**Figure S3.17.** Overlap of Differently expressed genes between DuoMYC **5** and Omomyc.

Table S3.1. List of differently expressed genes by DuoMYC **5**.

	baseMean	log2FoldChange	lfcSE	stat	pvalue	padj	Symbol
ENSG00000228502	231.5547249	-0.677149607	0.175663757	4.531418911	5.86E-06	0.000525138	EEF1A1P11
ENSG00000135766	403.3851924	0.933252167	0.134210772	-7.355808651	1.90E-13	8.29E-11	EGLN1
ENSG00000117318	1236.353667	-1.266326031	0.072314822	17.68951726	5.05E-70	5.81E-66	ID3
ENSG00000160752	655.050198	0.731286092	0.109907653	-7.059502655	1.67E-12	6.34E-10	FDPS
ENSG00000117407	248.5514861	0.767308133	0.172536598	-5.051097079	4.39E-07	5.68E-05	ARTN
ENSG00000163041	2828.281156	0.719232345	0.069166433	-10.66255483	1.52E-26	1.95E-23	H3-3A
ENSG00000188290	894.3050678	0.741488778	0.106500938	-7.342785815	2.09E-13	9.02E-11	HES4
ENSG00000237330	134.6474068	0.674830464	0.240622974	-3.702726004	0.000213295	0.010110427	RNF223
ENSG00000175793	9147.604108	0.695786348	0.0510936	-13.81885137	1.96E-43	4.84E-40	SFN
ENSG00000158246	278.4923329	0.504439113	0.150683882	-4.076257055	4.58E-05	0.002968624	TENT5B
ENSG00000179862	30.22672621	1.311533431	0.523204432	-3.53060123	0.000414616	0.017238048	CITED4
ENSG00000132196	681.7037312	0.51331035	0.09891238	-5.673164207	1.40E-08	2.83E-06	HSD17B7
ENSG00000131584	477.1327101	0.548440978	0.1087839	-5.548004472	2.89E-08	5.17E-06	ACAP3
ENSG00000049249	21.26720974	2.262926605	0.536276125	-4.855182655	1.20E-06	0.000130109	TNFRSF9
ENSG00000225630	437.7967628	-2.020114691	0.143036122	14.33872583	1.25E-46	3.33E-43	MTND2P28
ENSG00000237973	407.362517	-0.824833415	0.145208205	6.169319504	6.86E-10	1.88E-07	MTCO1P12
ENSG00000229344	185.5931859	-1.145975921	0.210961522	5.946025057	2.75E-09	6.54E-07	MTCO2P12
ENSG00000248527	1781.157201	-0.833244334	0.098892019	8.757352547	2.00E-18	1.50E-15	MTATP6P1
ENSG00000198744	170.8838661	-1.137922662	0.207389113	6.005658593	1.91E-09	4.70E-07	MTCO3P12
ENSG00000187017	1985.286462	0.513915333	0.062136749	-8.57799432	9.65E-18	6.94E-15	ESPN
ENSG00000177606	1266.27815	0.641782312	0.071079043	-9.330214581	1.06E-20	1.01E-17	JUN
ENSG00000169174	3659.335143	0.822508825	0.054132618	-15.37799939	2.30E-53	7.93E-50	PCSK9
ENSG00000162496	654.5403177	-0.617407556	0.098303862	6.703869775	2.03E-11	6.67E-09	DHRS3
ENSG00000235847	19.85093328	-1.440792589	0.572571089	3.551374032	0.000383225	0.016146937	LDHAP7
ENSG00000204253	186.1866783	-0.686735834	0.184504029	4.427765805	9.52E-06	0.000802772	HNRNPCP2
ENSG00000144485	1706.874218	0.707564086	0.096135567	-7.76474083	8.18E-15	4.48E-12	HES6
ENSG00000172478	10.8900887	2.351048971	0.908130673	-3.554414594	0.000378822	0.016000457	MAB21L4
ENSG00000134324	565.5613349	0.65954789	0.112912365	-6.295144476	3.07E-10	8.98E-08	LPIN1
ENSG00000234072	89.19256337	0.779827477	0.272330702	-3.75784314	0.000171384	0.008512625	GTF3C2-AS2
ENSG00000115738	144.755946	-1.117909847	0.194253884	6.244228329	4.26E-10	1.21E-07	ID2
ENSG00000249992	179.0815529	0.846531789	0.187447167	-5.118207528	3.08E-07	4.16E-05	TMEM158
ENSG00000169908	44.50603735	0.930551644	0.416724387	-3.352889775	0.000799725	0.028102777	TM4SF1
ENSG00000134107	1234.20519	0.502626991	0.073272862	-7.2136474	5.45E-13	2.24E-10	BHLHE40
ENSG00000239445	62.85871615	-0.66600084	0.311397261	3.255584236	0.001131593	0.03711884	ST3GAL6-AS1
ENSG00000163702	81.54184715	0.674508987	0.290636646	-3.365736578	0.000763396	0.027242254	IL17RC
ENSG00000230409	37.21282564	-1.093731168	0.391711152	3.73658901	0.000186533	0.00910452	TCEA1P2
ENSG00000136603	288.4785348	-0.575603253	0.155848314	4.368005051	1.25E-05	0.001010944	SKIL
ENSG00000164105	301.4180674	0.520749996	0.131494368	-4.586224556	4.51E-06	0.000422076	SAP30
ENSG00000137440	490.6230144	0.7298345	0.10878201	-7.112820795	1.14E-12	4.41E-10	FGFBP1
ENSG00000118804	17.69755514	1.37367076	0.651678075	-3.286197131	0.001015499	0.033956245	STBD1
ENSG00000052802	3597.584659	0.747231147	0.082911966	-9.283395917	1.64E-20	1.53E-17	MSMO1
ENSG00000196656	19.3129026	1.955555708	0.603070367	-4.033260388	5.50E-05	0.003476603	
ENSG00000184985	35.26930665	1.227631245	0.436303083	-3.745180457	0.000180264	0.008911971	SORCS2
ENSG00000164211	1336.956198	0.503337533	0.085795041	-6.280628834	3.37E-10	9.70E-08	STARD4
ENSG00000112972	4630.614605	0.85085904	0.052982972	-16.20790035	4.43E-59	2.19E-55	HMGCS1
ENSG00000131495	337.1190849	-0.525398196	0.139677273	4.4231345	9.73E-06	0.000814784	NDUFA2
ENSG00000185641	158.9857277	0.775444147	0.216242583	-4.321793199	1.55E-05	0.001205569	
ENSG00000251493	390.4288688	0.649297237	0.139581745	-5.221153847	1.78E-07	2.59E-05	FOXD1
ENSG00000113161	7902.393155	0.635040295	0.054034178	-11.92092139	9.21E-33	1.59E-29	HMGCR
ENSG00000169220	280.8266316	0.560284555	0.151090515	-4.386784622	1.15E-05	0.0009407	RGS14
ENSG00000247627	76.68076647	-0.862018172	0.295816911	3.807248642	0.000140521	0.007280952	MTND4P12
ENSG00000164292	2241.754531	-1.021702083	0.062146574	16.60938295	5.96E-62	3.43E-58	RHOBTB3
ENSG00000120437	1995.729373	0.839948482	0.07603561	-11.27925883	1.66E-29	2.49E-26	ACAT2
ENSG00000181577	445.4144633	0.935362788	0.118695429	-8.240298332	1.72E-16	1.08E-13	LINC03040
ENSG00000112559	443.3927042	0.509480573	0.148500378	-4.137180635	3.52E-05	0.002383691	MDFI
ENSG00000289047	122.8453228	-0.520167436	0.236040061	3.246248068	0.001169369	0.037961039	
ENSG00000186480	3416.231027	1.042626683	0.061379901	-17.15176476	6.10E-66	5.26E-62	INSIG1
ENSG00000130675	197.7197087	0.640560433	0.178368957	-4.306639049	1.66E-05	0.001276748	MNX1
ENSG00000196456	135.4419583	0.529680252	0.219300715	-3.383722963	0.000715101	0.025893716	ZNF775
ENSG00000001630	219.5760083	0.511500389	0.198274333	-3.491716916	0.000479927	0.019415366	CYP51A1
ENSG00000128564	982.4353783	0.760945056	0.089133467	-8.861212179	7.91E-19	6.35E-16	VGF
ENSG00000176532	65.62810358	0.96383906	0.319999316	-3.883038244	0.000103159	0.005788329	PRR15
ENSG00000146834	422.2659949	0.538594872	0.118293774	-5.102191798	3.36E-07	4.47E-05	MEPCE
ENSG00000228668	6.91861558	3.103096778	1.310730062	-3.183164159	0.00145675	0.044843469	TRGV5P
ENSG00000147155	751.8149689	0.63192932	0.09032721	-7.378386645	1.60E-13	7.09E-11	EBP
ENSG00000232024	25.84236448	-1.269086299	0.552823293	3.407710023	0.000655105	0.024362564	LSM12P1
ENSG00000182759	90.11865355	0.935909029	0.274786828	-4.194243106	2.74E-05	0.001916379	MAFA
ENSG00000204839	1027.140792	0.540995076	0.082970868	-6.904555227	5.04E-12	1.79E-09	MROH6
ENSG00000179886	444.8976757	0.585313812	0.114257648	-5.626189672	1.84E-08	3.49E-06	TIGD5
ENSG00000079459	10204.90465	0.73319437	0.043463459	-16.98483193	1.06E-64	7.34E-61	FDFT1
ENSG00000198576	284.5964799	0.505938226	0.149902911	-4.094605763	4.23E-05	0.002800959	ARC
ENSG00000198435	715.8546023	0.533436704	0.095770476	-6.026820952	1.67E-09	4.18E-07	NRARP
ENSG00000167106	595.3319625	0.903537742	0.100195605	-9.33768241	9.85E-21	9.71E-18	EEIG1
ENSG00000160326	529.5893848	0.540866566	0.114675099	-5.252097717	1.50E-07	2.22E-05	SLC2A6
ENSG00000167136	532.4850942	0.647826541	0.115091265	-6.097003748	1.08E-09	2.85E-07	ENDOG
ENSG00000173457	5961.409218	0.738188416	0.064528473	-11.64172785	2.53E-31	3.97E-28	PPP1R14B
ENSG00000171219	605.5795648	0.534577677	0.107304783	-5.487497089	4.08E-08	7.07E-06	CDC42BPG
ENSG00000175602	2609.522732	0.597756331	0.085621112	-7.322728804	2.43E-13	1.04E-10	CCDC85B
ENSG00000188070	402.6203549	0.634770101	0.129442656	-5.442694874	5.25E-08	8.71E-06	ZFTA
ENSG00000184545	154.8136315	0.909819066	0.179472045	-5.611875785	2.00E-08	3.73E-06	DUSP8
ENSG00000167799	184.8800561	0.566006883	0.196052802	-3.734183227	0.000188325	0.009166053	NUDT8
ENSG00000244398	169.3144301	0.619893668	0.235263741	-3.567168307	0.00036086	0.015392518	RPL36AP37
ENSG00000168040	231.9496178	0.775876806	0.175838694	-5.017960955	5.22E-07	6.58E-05	FADD
ENSG00000172893	6668.327026	0.519921593	0.044632961	-11.86271887	1.85E-32	3.04E-29	DHCR7
ENSG00000149809	1200.360055	0.724072154	0.098170722	-7.719824881	1.16E-14	6.18E-12	TM7SF2
ENSG00000170955	170.4560238	0.843828676	0.208020789	-4.71878638	2.37E-06	0.000239392	CAVIN3
ENSG00000173599	622.366466	0.595534163	0.106380186	-6.058473172	1.37E-09	3.54E-07	PC
ENSG00000213260	17.26152316	-1.728144374	0.621814571	3.737778425	0.000185653	0.009074404	YWHAZP5
ENSG00000122861	3021.610212	0.506620584	0.056482904	-9.250697579	2.23E-20	2.03E-17	PLAU
ENSG00000107954	161.6353167	0.63224472	0.194707984	-4.028734102	5.61E-05	0.003537732	NEURL1
ENSG00000120549	164.7803085	0.573112587	0.195120352	-3.771393178	0.000162339	0.00821405	KIAA1217
ENSG00000077150	2283.218521	0.564197369	0.063164107	-9.221404461	2.93E-20	2.59E-17	NFKB2
ENSG00000110921	1578.739633	0.73875439	0.067910863	-11.12875848	9.09E-29	1.25E-25	MVK
ENSG00000167552	6362.891955	0.507618101	0.062671572	-8.383732489	5.13E-17	3.40E-14	TUBA1A
ENSG00000185950	902.5375034	0.609734254	0.09401347	-6.885875	5.74E-12	2.02E-09	IRS2
ENSG00000293057	91.71816609	-1.305444789	0.26467505	5.510384959	3.58E-08	6.27E-06	
ENSG00000257179	24.9360431	-1.621315591	0.480905292	4.181472849	2.90E-05	0.002006916	HMGN2P6
ENSG00000165804	545.4379426	0.556964426	0.112788186	-5.457480112	4.83E-08	8.13E-06	ZNF219
ENSG00000259020	44.37911172	-2.045641828	0.387820987	5.813559753	6.12E-09	1.38E-06	
ENSG00000100836	91.47722244	0.630260242	0.288475017	-3.269641279	0.001076839	0.035696039	PABPN1

Table S3.1. List of differently expressed genes by DuoMYC **5**.

	baseMean	log2FoldChange	lfcSE	stat	pvalue	padj	Symbol
ENSG00000232573	232.8337439	0.901028106	0.18626645	-5.405177638	6.47E-08	1.04E-05	RPL3P4
ENSG00000137825	393.2801852	0.552878362	0.120590614	-5.140241663	2.74E-07	3.80E-05	ITPKA
ENSG00000256338	110.647322	-0.841577214	0.222730363	4.479995705	7.46E-06	0.000645258	RPL41P2
ENSG00000234797	196.4322686	-0.82276851	0.168917368	5.436753178	5.43E-08	8.96E-06	RPS3AP6
ENSG00000138623	395.3797771	0.573130199	0.125978138	-5.120354885	3.05E-07	4.14E-05	SEMA7A
ENSG00000140264	1461.09599	-0.548008471	0.082334272	7.042658889	1.89E-12	7.07E-10	SERF2
ENSG00000135736	216.7870469	0.509217324	0.162165555	-3.908143019	9.30E-05	0.005358144	CCDC102A
ENSG00000126603	260.3455188	0.502988139	0.154398444	-3.999882965	6.34E-05	0.003912171	GLIS2
ENSG00000158792	1105.761719	0.564869922	0.081321421	-7.3210941	2.46E-13	1.04E-10	SPATA2L
ENSG00000227827	127.5358408	0.841754912	0.222910466	-4.479976753	7.47E-06	0.000645258	PKD1P2
ENSG00000179588	345.2915684	0.524022343	0.135768688	-4.499660539	6.81E-06	0.000603775	ZFPM1
ENSG00000167508	4376.647092	1.140927141	0.056159148	-20.41087406	1.34E-92	4.62E-88	MVD
ENSG00000184207	1756.648795	0.551605398	0.075881496	-7.62511121	2.44E-14	1.24E-11	PGP
ENSG00000183971	2716.585436	0.679375601	0.068581331	-10.17938612	2.45E-24	2.82E-21	NPW
ENSG00000121104	486.593292	0.560913164	0.106006788	-5.7758906	7.65E-09	1.67E-06	FAM117A
ENSG00000189343	924.790806	0.818684267	0.19581988	-4.840769797	1.29E-06	0.000138608	RPS2P46
ENSG00000109107	985.9506263	0.566604888	0.078288483	-7.603957215	2.87E-14	1.42E-11	ALDOC
ENSG00000068137	713.410686	0.593336772	0.095612544	-6.630419863	3.35E-11	1.09E-08	PLEKHH3
ENSG00000185813	1693.42127	0.579434301	0.064082242	-9.339762035	9.66E-21	9.71E-18	PCYT2
ENSG00000161682	704.5112821	0.604801591	0.09304567	-6.904926245	5.02E-12	1.79E-09	FAM171A2
ENSG00000169710	47793.43142	0.591668505	0.038730423	-14.97576923	1.06E-50	3.32E-47	FASN
ENSG00000212724	269.1398349	0.569852639	0.149361582	-4.480927491	7.43E-06	0.000645258	KRTAP2-3
ENSG00000136463	276.5510604	0.529242368	0.140814991	-4.412773639	1.02E-05	0.000848603	TACO1
ENSG00000130584	122.9082355	0.642198043	0.250461808	-3.519996466	0.000431553	0.017792133	ZBTB46
ENSG00000125968	1551.855576	-1.15223023	0.074701448	15.61537494	5.72E-55	2.19E-51	ID1
ENSG00000172216	868.7133666	0.591211364	0.091770483	-6.842064554	7.81E-12	2.72E-09	CEBPB
ENSG00000227063	414.1756969	0.507738825	0.159816365	-3.935532181	8.30E-05	0.004921987	RPL41P1
ENSG00000088766	247.0165799	1.100125637	0.168779921	-6.948802058	3.68E-12	1.35E-09	CRLS1
ENSG00000131069	1400.502519	0.834006505	0.0695881	-12.21964967	2.44E-34	4.43E-31	ACSS2
ENSG00000160951	81.6317488	1.032413114	0.272725266	-4.504366469	6.66E-06	0.000592072	PTGER1
ENSG00000142279	276.9560526	0.557655715	0.152761387	-4.337922139	1.44E-05	0.001138416	WTIP
ENSG00000160469	163.4458425	0.639410596	0.197321059	-4.022756304	5.75E-05	0.003615546	BRSK1
ENSG00000197380	82.71752111	0.586888524	0.288443338	-3.167516254	0.001537471	0.046480584	DACT3
ENSG00000233493	248.0456034	1.307459463	0.170419189	-8.04440388	8.67E-16	5.16E-13	TMEM238
ENSG00000108106	8307.44442	0.667583626	0.055289693	-12.29093759	1.01E-34	1.94E-31	UBE2S
ENSG00000130522	3876.91953	1.059266613	0.054681683	-19.52185632	7.16E-85	1.24E-80	JUND
ENSG00000129968	2197.557767	0.616371871	0.07227457	-8.839945374	9.58E-19	7.51E-16	ABHD17A
ENSG00000213638	222.0524333	0.582457966	0.162152454	-4.296956354	1.73E-05	0.001324918	ADAT3
ENSG00000171223	1547.507543	0.54413062	0.069917823	-8.115129849	4.85E-16	2.94E-13	JUNB
ENSG00000141933	318.6311258	1.177675967	0.139245913	-8.794602353	1.44E-18	1.10E-15	TPGS1
ENSG00000174951	453.0068486	0.533843069	0.113565591	-5.230734911	1.69E-07	2.47E-05	FUT1
ENSG00000130203	2861.890541	0.58315692	0.067560961	-8.922756196	4.55E-19	3.74E-16	APOE
ENSG00000104881	334.2703606	0.503048617	0.134954026	-4.383339071	1.17E-05	0.000953449	PPP1R13L
ENSG00000181588	1949.959942	0.595031888	0.062504375	-9.798276509	1.15E-22	1.20E-19	MEX3D
ENSG00000142235	214.5983803	0.871407207	0.166125128	-5.76712887	8.06E-09	1.74E-06	LMTK3
ENSG00000142544	753.3707306	0.696970692	0.090690168	-8.037078751	9.20E-16	5.38E-13	CTU1
ENSG00000171119	219.2310769	0.511406013	0.185821018	-3.616783974	0.000298286	0.013272904	NRTN
ENSG00000115286	74.04604345	-0.847792303	0.276452551	3.920981336	8.82E-05	0.005149288	NDUFS7
ENSG00000070404	539.0006092	0.55144177	0.105537949	-5.713775467	1.10E-08	2.28E-06	FSTL3
ENSG00000063169	291.8908586	0.542993624	0.14685976	-4.365563944	1.27E-05	0.001018163	BICRA
ENSG00000176531	340.0521146	0.591104899	0.127046993	-5.206620322	1.92E-07	2.78E-05	PHLDB3
ENSG00000099625	436.676006	0.626729185	0.14156248	-5.016857464	5.25E-07	6.59E-05	CBARP
ENSG00000130751	90.39282556	0.649548988	0.273778218	-3.396069031	0.000683611	0.024989464	NPAS1
ENSG00000130748	717.6072024	0.65642527	0.114808134	-6.181060391	6.37E-10	1.77E-07	TMEM160
ENSG00000105327	599.443056	0.633009335	0.113432105	-6.052980165	1.42E-09	3.63E-07	BBC3
ENSG00000104856	768.9317272	0.555665945	0.104308584	-5.807617707	6.34E-09	1.41E-06	RELB
ENSG00000087074	1136.377849	0.547651084	0.085315419	-6.819431634	9.14E-12	3.15E-09	PPP1R15A
ENSG00000105376	324.7828012	0.700778117	0.133324951	-5.771414449	7.86E-09	1.71E-06	ICAM5
ENSG00000130164	3325.454457	0.769860787	0.053266305	-14.6419108	1.52E-48	4.36E-45	LDLR
ENSG00000118046	2148.531028	0.518546403	0.066547737	-8.120587584	4.64E-16	2.86E-13	STK11
ENSG00000128346	13.6013708	1.652585146	0.83207299	-3.21116497	0.00132198	0.041890627	C22orf23
ENSG00000234965	293.1512178	1.174382018	0.145638734	-8.415583351	3.91E-17	2.65E-14	SHISA8
ENSG00000244486	44.79138268	0.812639739	0.426851777	-3.146761154	0.001650898	0.04885864	SCARF2
ENSG00000250479	2190.047135	0.546703684	0.063099844	-8.964597805	3.11E-19	2.62E-16	CHCHD10
ENSG00000241360	338.471307	1.045647469	0.149064821	-7.417498626	1.19E-13	5.35E-11	PDXP
ENSG00000100078	387.3853599	0.937269127	0.132515931	-7.468655072	8.10E-14	3.73E-11	PLA2G3
ENSG00000188064	466.6501608	0.517882353	0.111172297	-5.194358499	2.05E-07	2.94E-05	WNT7B
ENSG00000198911	6478.286562	0.559946447	0.044293	-12.82421532	1.20E-37	2.59E-34	SREBF2
ENSG00000251322	860.8463556	0.599024279	0.088032157	-7.190236277	6.47E-13	2.63E-10	SHANK3
ENSG00000100290	442.9782556	1.403386766	0.113355425	-12.61421942	1.76E-36	3.58E-33	BIK
ENSG00000160285	2461.560651	1.07421771	0.067152491	-16.17184648	7.97E-59	3.44E-55	LSS
ENSG00000198888	13159.48781	-0.594063615	0.132465423	5.33225338	9.70E-08	1.51E-05	MT-ND1
ENSG00000198763	26614.62814	-0.702079284	0.136677877	5.383596506	7.30E-08	1.17E-05	MT-ND2
ENSG00000198804	94865.41161	-0.869397801	0.06378354	12.82849767	1.14E-37	2.59E-34	MT-CO1
ENSG00000198712	53617.40817	-0.859431899	0.110706169	7.891463143	2.99E-15	1.69E-12	MT-CO2
ENSG00000228253	171.9837818	-0.603822747	0.24460751	3.45289859	0.000554597	0.021673895	MT-ATP8
ENSG00000198899	28157.53597	-0.850358629	0.124885797	7.50824485	5.99E-14	2.79E-11	MT-ATP6
ENSG00000198938	49873.0884	-0.753901247	0.107608368	7.640688901	2.16E-14	1.11E-11	MT-CO3
ENSG00000198886	64138.84252	-0.713868051	0.125229429	7.063623356	1.62E-12	6.22E-10	MT-ND4
ENSG00000198786	22948.29882	-0.756262868	0.162043474	5.164754651	2.41E-07	3.38E-05	MT-ND5
ENSG00000198695	8257.40849	-0.755124321	0.110516185	7.222223208	5.11E-13	2.13E-10	MT-ND6
ENSG00000198727	24903.58321	-0.813565197	0.14369152	5.81970741	5.90E-09	1.35E-06	MT-CYB

Table S3.2. List of differently expressed genes by Omomyc.

	baseMean	log2FoldChange	lfcSE	stat	pvalue	padj	Symbol
ENSG00000228502	231.5547249	-0.906950305	0.171412268	5.814086253	6.10E-09	4.10E-07	EEF1A1P11
ENSG00000135766	403.3851924	0.88130259	0.133652286	-7.010836275	2.37E-12	3.17E-10	EGLN1
ENSG00000117318	1236.353667	-1.18598749	0.071055122	16.87507041	6.86E-64	2.48E-60	ID3
ENSG00000162522	2238.690773	0.589747583	0.074595268	-8.230933882	1.86E-16	4.37E-14	NHSL3
ENSG00000117407	248.5514861	0.586543662	0.176160581	-4.070260406	4.70E-05	0.000704634	ARTN
ENSG00000228594	231.7405887	0.508312429	0.164995471	-3.839645522	0.000123212	0.00154477	FNDC10
ENSG00000224114	98.69811744	-0.632183514	0.363991443	3.025097505	0.00248553	0.016114048	
ENSG00000163041	2828.281156	0.738040275	0.068838184	-10.97449635	5.07E-28	2.61E-25	H3-3A
ENSG00000237330	134.6474068	0.611026073	0.24230234	-3.472878634	0.000514908	0.004735144	RNF223
ENSG00000185519	226.3217743	0.503925706	0.163600806	-3.83547857	0.00012532	0.001564046	FAM131C
ENSG00000263528	79.07064158	0.715278515	0.279443144	-3.524583256	0.00042415	0.00408065	IKBKE
ENSG00000160094	204.6155299	0.574808054	0.161695161	-4.245579877	2.18E-05	0.000380339	ZNF362
ENSG00000175793	9147.604108	0.556930207	0.051128941	-11.12758749	9.21E-29	4.99E-26	SFN
ENSG00000158246	278.4923329	0.558307608	0.147181232	-4.440390594	8.98E-06	0.000187791	TENT5B
ENSG00000132196	681.7037312	0.580620736	0.097312865	-6.393763561	1.62E-10	1.65E-08	HSD17B7
ENSG00000204060	128.5879628	0.770803946	0.213441226	-4.334099757	1.46E-05	0.000281615	FOXO6
ENSG00000225630	437.7967628	-1.617167301	0.138655084	11.91286872	1.01E-32	6.46E-30	MTND2P28
ENSG00000198744	170.8838661	-0.763131266	0.207633863	4.392058085	1.12E-05	0.00022821	MTCO3P12
ENSG00000158292	291.749485	0.700976005	0.132176948	-5.801168254	6.59E-09	4.36E-07	GPR153
ENSG00000169174	3659.335143	0.767210323	0.053957359	-14.41319606	4.27E-47	5.79E-44	PCSK9
ENSG00000116133	12856.50025	0.537091876	0.043835385	-12.45946642	1.24E-35	9.61E-33	DHCR24
ENSG00000204253	186.1866783	-0.942485225	0.179640285	5.778163656	7.55E-09	4.90E-07	HNRNPCP2
ENSG00000144485	1706.874218	0.50081256	0.097027796	-5.630429478	1.80E-08	1.05E-06	HES6
ENSG00000234072	89.19256337	0.605385153	0.285947735	-3.207735688	0.001337844	0.010078486	GTF3C2-AS2
ENSG00000115738	144.755946	-0.896210776	0.191146908	5.279089017	1.30E-07	5.81E-06	ID2
ENSG00000249992	179.0815529	0.699250062	0.189615198	-4.387373688	1.15E-05	0.000232009	TMEM158
ENSG00000137440	490.6230144	0.751670567	0.107535836	-7.375947996	1.63E-13	2.64E-11	FGFBP1
ENSG00000178458	793.0581631	0.515790618	0.107036529	-5.324061782	1.01E-07	4.76E-06	H3P16
ENSG00000052802	3597.584659	0.593674364	0.083215228	-7.452549207	9.16E-14	1.63E-11	MSMO1
ENSG00000123933	1325.123198	0.586206096	0.078140424	-7.843207992	4.39E-15	9.15E-13	MXD4
ENSG00000249855	104.4959411	-0.702634314	0.267385541	3.576001644	0.000348889	0.003496318	EEF1A1P19
ENSG00000112972	4630.614605	0.554045444	0.053200247	-10.63900081	1.96E-26	9.66E-24	HMGCS1
ENSG00000131495	337.1190849	-0.716364011	0.136260931	5.766517891	8.09E-09	5.22E-07	NDUFA2
ENSG00000164438	101.5774309	0.610999573	0.25941726	-3.359517071	0.000780788	0.006506369	TLX3
ENSG00000185641	158.9857277	0.785281547	0.213613087	-4.383872513	1.17E-05	0.000233889	
ENSG00000251493	390.4288688	0.672104692	0.137979958	-5.410512843	6.28E-08	3.26E-06	FOXD1
ENSG00000250182	342.7482363	-0.593239224	0.157469266	4.433496156	9.27E-06	0.000192415	EEF1A1P13
ENSG00000164292	2241.754531	-0.780643081	0.06119767	12.97486806	1.70E-38	1.67E-35	RHOBTB3
ENSG00000120437	1995.729373	0.597494084	0.076416615	-8.118119504	4.73E-16	1.07E-13	ACAT2
ENSG00000181577	445.4144633	1.109683485	0.116557978	-9.818823255	9.34E-23	3.49E-20	LINC03040
ENSG00000135604	85.39272502	0.537511112	0.27994605	-3.063430349	0.002188151	0.014605203	STX11
ENSG00000186480	3416.231027	0.841092239	0.061423884	-13.88868561	7.42E-44	8.93E-41	INSIG1
ENSG00000165215	241.218457	0.640856719	0.182052749	-4.228940578	2.35E-05	0.00040502	CLDN3
ENSG00000189143	1882.415566	0.522935654	0.062549369	-8.640023601	5.62E-18	1.56E-15	CLDN4
ENSG00000050327	348.4882086	0.51549062	0.129849225	-4.581049477	4.63E-06	0.000110151	ARHGEF5
ENSG00000130675	197.7197087	0.527560846	0.180725343	-3.72374625	0.000196288	0.002235105	MNX1
ENSG00000128564	982.4353783	0.608741979	0.08931285	-7.197428441	6.14E-13	9.11E-11	VGF
ENSG00000009950	110.6217194	0.771747015	0.236576291	-4.055253821	5.01E-05	0.000738116	MLXIPL
ENSG00000198910	505.385481	0.533824752	0.121513711	-4.951275552	7.37E-07	2.42E-05	L1CAM
ENSG00000182759	90.11865355	0.793191469	0.280542476	-3.730791619	0.000190879	0.002184072	MAFA
ENSG00000179886	444.8976757	0.620059385	0.112588549	-5.975663898	2.29E-09	1.77E-07	TIGD5
ENSG00000187954	204.5359387	0.540043744	0.165930308	-3.992974471	6.52E-05	0.000910888	ZFTRAF1
ENSG00000079459	10204.90465	0.67112732	0.043397678	-15.56730061	1.21E-54	2.19E-51	FDFT1
ENSG00000275342	1395.427567	0.527672073	0.081335239	-6.861714135	6.80E-12	8.64E-10	PRAG1
ENSG00000198576	284.5964799	0.501887162	0.148036119	-4.088318006	4.35E-05	0.000663279	ARC
ENSG00000198435	715.8546023	0.536552605	0.094799899	-6.100139012	1.06E-09	8.76E-08	NRARP
ENSG00000160326	529.5893848	0.695840265	0.111833283	-6.641235207	3.11E-11	3.58E-09	SLC2A6
ENSG00000196358	126.8372484	1.03673489	0.223892372	-5.221906594	1.77E-07	7.43E-06	NTNG2
ENSG00000173457	5961.409218	0.529501713	0.064786365	-8.42033694	3.75E-17	9.46E-15	PPP1R14B
ENSG00000181649	3156.996748	0.537570666	0.052842471	-10.35745393	3.87E-25	1.68E-22	PHLDA2
ENSG00000175567	112.8095575	0.535132572	0.255078218	-3.167317448	0.001538523	0.011246165	UCP2
ENSG00000129757	438.4045358	0.696116286	0.121029272	-6.196050315	5.79E-10	5.23E-08	CDKN1C
ENSG00000172893	6668.327026	0.586128051	0.044360731	-13.39530209	6.44E-41	6.98E-38	DHCR7
ENSG00000149809	1200.360055	0.895542308	0.096889157	-9.527410784	1.61E-21	5.29E-19	TM7SF2
ENSG00000173599	622.366466	0.623934549	0.10514343	-6.377334626	1.80E-10	1.82E-08	PC
ENSG00000181274	174.9348825	0.521627324	0.185558598	-3.64051627	0.000272092	0.002873119	FRAT2
ENSG00000107954	161.6353167	0.734805746	0.188386772	-4.571625579	4.84E-06	0.000113971	NEURL1
ENSG00000099194	35425.96812	0.576931618	0.045842619	-12.75490059	2.93E-37	2.44E-34	SCD
ENSG00000111319	942.3544039	0.626237262	0.091282085	-7.232159573	4.75E-13	7.15E-11	SCNN1A
ENSG00000186897	223.4724216	0.543357122	0.163867574	-4.036031853	5.44E-05	0.000784171	C1QL4
ENSG00000110921	1578.739633	0.687627726	0.067565519	-10.43792266	1.66E-25	7.51E-23	MVK
ENSG00000135114	133.3675076	0.504943616	0.219929538	-3.275750843	0.001053815	0.008289694	OASL
ENSG00000159335	7276.9351	0.56522062	0.04972025	-11.58685936	4.80E-31	2.89E-28	PTMS
ENSG00000167588	100.4517483	-0.796893059	0.222089366	4.320415823	1.56E-05	0.000294846	GPD1
ENSG00000167552	6362.891955	0.597228892	0.062332335	-9.797084653	1.16E-22	4.05E-20	TUBA1A
ENSG00000185950	902.5375034	0.552766045	0.093740836	-6.319230855	2.63E-10	2.61E-08	IRS2
ENSG00000293057	91.71816609	-1.755344008	0.263039813	7.103416663	1.22E-12	1.67E-10	
ENSG00000165804	545.4379426	0.539755071	0.111897507	-5.326649483	1.00E-07	4.71E-06	ZNF219
ENSG00000133935	1950.67499	0.534006255	0.071597197	-7.765062574	8.16E-15	1.61E-12	ERG28
ENSG00000232573	232.8337439	0.808551252	0.186703356	-4.93720715	7.92E-07	2.56E-05	RPL3P4
ENSG00000276168	300.8779606	0.621753463	0.157679185	-4.585201677	4.54E-06	0.000109184	RN7SL1
ENSG00000136378	180.395016	0.573010506	0.178706173	-3.96454255	7.35E-05	0.001008385	ADAMTS7
ENSG00000256338	110.647322	-0.995135337	0.217430837	5.181120774	2.21E-07	9.02E-06	RPL41P2
ENSG00000234797	196.4322686	-0.930265672	0.165968877	6.102918221	1.04E-09	8.75E-08	RPS3AP6
ENSG00000140264	1461.09599	-0.691512223	0.081589257	8.795476904	1.42E-18	4.29E-16	SERF2
ENSG00000204991	361.7753124	0.505743191	0.128676312	-4.540925637	5.60E-06	0.000128273	SPIRE2
ENSG00000118898	768.0483567	0.538475023	0.114666593	-5.213588072	1.85E-07	7.69E-06	PPL
ENSG00000179588	345.2915684	0.751557518	0.130455455	-6.225328818	4.81E-10	4.49E-08	ZFPM1
ENSG00000167508	4376.647092	0.969176323	0.056119594	-17.42899484	4.97E-68	2.69E-64	MVD
ENSG00000008710	248.0056433	0.509367243	0.179022395	-3.663277664	0.000249008	0.002680889	PKD1
ENSG00000103495	275.9037838	0.595242997	0.153752796	-4.518987053	6.21E-06	0.000139652	MAZ
ENSG00000183971	2716.585436	0.555463959	0.068619188	-8.404563463	4.29E-17	1.06E-14	NPW
ENSG00000196557	720.954687	0.529418791	0.089827481	-6.316151648	2.68E-10	2.64E-08	CACNA1H
ENSG00000121104	486.593292	0.662432996	0.103758157	-6.799366209	1.05E-11	1.26E-09	FAM117A
ENSG00000131094	125.9100296	0.750321331	0.209035563	-4.312063471	1.62E-05	0.000304185	C1QL1
ENSG00000189343	924.790806	0.778801368	0.19612932	-4.671694498	2.99E-06	7.76E-05	RPS2P46
ENSG00000109107	985.9506263	0.562928272	0.07753852	-7.620008514	2.54E-14	4.74E-12	ALDOC
ENSG00000185813	1693.42127	0.605898229	0.063479495	-9.811538676	1.00E-22	3.63E-20	PCYT2
ENSG00000161682	704.5112821	0.729277421	0.091313722	-8.324412069	8.47E-17	2.04E-14	FAM171A2
ENSG00000169710	47793.43142	0.652561398	0.038627948	-16.74332719	6.33E-63	1.72E-59	FASN
ENSG00000212901	610.0331719	-0.534879493	0.128658651	4.752246159	2.01E-06	5.60E-05	KRTAP3-1
ENSG00000006283	99.86910272	0.732852761	0.258007829	-3.729111402	0.000192156	0.00219581	CACNA1G
ENSG00000101493	553.4924869	0.516593201	0.10015384	-5.634737042	1.75E-08	1.04E-06	ZNF516
ENSG00000101132	847.2085792	-0.614021982	0.130217591	5.280997905	1.28E-07	5.80E-06	PFDN4
ENSG00000130702	341.354272	0.598497283	0.140407938	-4.858367232	1.18E-06	3.62E-05	LAMA5
ENSG00000130584	122.9082355	0.636808281	0.247423887	-3.511913412	0.000444893	0.004215488	ZBTB46
ENSG00000125968	1551.855576	-0.885729368	0.073442429	12.29435998	9.71E-35	6.58E-32	ID1
ENSG00000177732	1972.206033	0.634888761	0.067076952	-9.7371526	2.09E-22	7.09E-20	SOX12
ENSG00000172216	868.7133666	0.565383697	0.091200911	-6.601876723	4.06E-11	4.53E-09	CEBPB
ENSG00000227063	414.1756969	0.527910961	0.157547558	-4.079821446	4.51E-05	0.000682634	RPL41P1
ENSG00000088766	247.0165799	0.534647272	0.179790238	-3.775216621	0.000159869	0.001893903	CRLS1

Table S3.2 List of differently expressed genes by Omomyc.

	baseMean	log2FoldChange	lfcSE	stat	pvalue	padj	Symbol
ENSG00000131069	1400.502519	0.837906692	0.069046898	-12.36570198	4.01E-35	2.89E-32	ACSS2
ENSG00000099864	685.5219725	0.5091333	0.097113591	-5.710562203	1.13E-08	7.05E-07	PALM
ENSG00000160951	81.6317488	0.863361897	0.277952186	-3.940853437	8.12E-05	0.00109126	PTGER1
ENSG00000160469	163.4458425	0.590292557	0.197197501	-3.808537034	0.000139791	0.001714192	BRSK1
ENSG00000233493	248.0456034	1.236094604	0.16980363	-7.664697202	1.79E-14	3.47E-12	TMEM238
ENSG00000108106	8307.44442	0.57142213	0.055290247	-10.52573051	3.86E-26	1.82E-23	UBE2S
ENSG00000130522	3876.91953	1.0442947	0.054462921	-19.32214537	3.50E-83	3.79E-79	JUND
ENSG00000133250	221.0634428	0.541373298	0.187217933	-3.713783828	0.000204183	0.002796902	ZNF414
ENSG00000129968	2197.557767	0.595902889	0.071971195	-8.583869058	9.17E-18	2.37E-15	ABHD17A
ENSG00000183248	144.5506403	0.755187554	0.203935862	-4.408567286	1.04E-05	0.000213494	PRR36
ENSG00000141933	318.6311258	0.760094178	0.14215349	-5.845914668	5.04E-09	3.50E-07	TPGS1
ENSG00000177051	576.5200848	0.502006229	0.104797286	-5.297823386	1.17E-07	5.33E-06	FBXO46
ENSG00000104881	334.2703606	0.66762989	0.130271707	-5.638074052	1.72E-08	1.02E-06	PPP1R13L
ENSG00000079432	1352.873251	0.513385951	0.090304717	-6.124888492	9.07E-10	7.68E-08	CIC
ENSG00000129946	88.89869943	0.893627602	0.266490694	-4.138669722	3.49E-05	0.000552444	SHC2
ENSG00000181588	1949.959942	0.527260426	0.062260946	-8.777524292	1.67E-18	4.89E-16	MEX3D
ENSG00000142235	214.5983803	0.879649279	0.164346406	-5.860916505	4.60E-09	3.24E-07	LMTK3
ENSG00000063169	291.8908586	0.604623914	0.143553148	-4.81462445	1.47E-06	4.33E-05	BICRA
ENSG00000130513	6882.632022	0.548477768	0.049323752	-11.3591096	6.68E-30	3.81E-27	GDF15
ENSG00000099625	436.676006	0.671478985	0.13962633	-5.351921952	8.70E-08	4.23E-06	CBARP
ENSG00000105327	599.443056	0.654850899	0.112312045	-6.280274272	3.38E-10	3.21E-08	BBC3
ENSG00000069399	336.5760576	0.682579507	0.122636486	-6.041389237	1.53E-09	1.23E-07	BCL3
ENSG00000261221	468.7050989	0.510145163	0.110714538	-5.134821668	2.82E-07	1.10E-05	ZNF865
ENSG00000130164	3325.454457	0.668574957	0.053150449	-12.78996134	1.87E-37	1.68E-34	LDLR
ENSG00000100330	87.01161036	0.661472467	0.258921914	-3.505408619	0.000455907	0.004294644	MTMR3
ENSG00000099889	234.9609478	0.589859533	0.159969146	-4.357310992	1.32E-05	0.00025747	ARVCF
ENSG00000234965	293.1512178	1.112013915	0.14494194	-8.038645578	9.08E-16	2.01E-13	SHISA8
ENSG00000250479	2190.047135	0.616061041	0.06246946	-10.12823168	4.14E-24	1.66E-21	CHCHD10
ENSG00000241360	338.471307	0.938005482	0.149023281	-6.737335029	1.61E-11	1.92E-09	PDXP
ENSG00000100078	387.3853599	0.940378875	0.131443023	-7.542309182	4.62E-14	8.34E-12	PLA2G3
ENSG00000188064	466.6501608	0.661741866	0.108230058	-6.544181969	5.98E-11	6.55E-09	WNT7B
ENSG00000198911	6478.286562	0.630593385	0.044014391	-14.49591063	1.29E-47	1.99E-44	SREBF2
ENSG00000251322	860.8463556	0.642813357	0.087013277	-7.768487962	7.94E-15	1.59E-12	SHANK3
ENSG00000160285	2461.560651	1.032158319	0.066919235	-15.60368063	6.87E-55	1.49E-51	LSS

Table S3.3 Significantly differently expressed pathways by DuoMYC **5**

	Term	ES	NES	NOM p-val	FDR q-val	FWER p-val	Tag %	Gene %
0	Cholesterol Homeostasis	-0.82591	-2.70139	0	0	0	43/71	9.18%
1	TNF-alpha Signaling via NF-kB	-0.66797	-2.47178	0	0	0	79/191	9.98%
2	Protein Secretion	0.600019	2.2817	0	0	0	45/94	11.56%
3	Hypoxia	-0.58229	-2.1561	0	0	0	61/197	10.27%
4	Myogenesis	-0.59031	-2.1455	0	0	0	68/186	14.58%
5	Apoptosis	-0.51435	-1.8545	0	0.000221	0.001	57/153	15.32%
7	Estrogen Response Early	-0.48117	-1.77126	0	0.000552	0.003	71/191	15.06%
6	G2-M Checkpoint	0.436277	1.806425	0	0.001127	0.003	74/199	12.53%
8	Androgen Response	-0.49545	-1.69233	0.001475	0.002525	0.014	14/96	3.31%
9	Estrogen Response Late	-0.43921	-1.62558	0.002639	0.004418	0.03	44/182	9.68%
11	TGF-beta Signaling	0.441022	1.501438	0.027933	0.010767	0.043	jnl-53	0.44%
10	Mitotic Spindle	-0.40223	-1.51045	0.006649	0.015954	0.121	67/199	14.97%
13	IL-6/JAK/STAT3 Signaling	-0.43601	-1.43656	0.024578	0.025806	0.223	30/77	19.89%
12	Adipogenesis	-0.38988	-1.43658	0.006757	0.028276	0.222	51/192	14.51%
14	DNA Repair	0.333783	1.351208	0.011152	0.032113	0.153	32/148	6.80%

Table S3.4 Significantly differently expressed pathways by Omomyc

	Term	ES	NES	NOM p-val	FDR q-val	FWER p-val	Tag %	Gene %
0	Cholesterol Homeostasis	-0.80753	-2.71233	0	0	0	33/71	5.10%
1	G2-M Checkpoint	0.567371	2.331756	0	0	0	98/199	11.29%
2	Myogenesis	-0.57259	-2.19715	0	0	0	61/186	12.54%
3	TNF-alpha Signaling via NF-kB	-0.57255	-2.19688	0	0	0	86/191	16.26%
4	Estrogen Response Early	-0.55963	-2.12312	0	0	0	81/191	14.43%
5	Protein Secretion	0.546611	2.028327	0	0	0	48/94	17.15%
6	DNA Repair	0.504444	1.976716	0	0	0	57/148	11.31%
7	Hypoxia	-0.50292	-1.95086	0	0.000253	0.001	58/197	13.44%
8	Estrogen Response Late	-0.47198	-1.77545	0	0.001897	0.007	59/182	11.83%
9	Apoptosis	-0.42526	-1.59697	0.001639	0.007045	0.036	44/153	11.38%
11	Mitotic Spindle	-0.40772	-1.56464	0	0.007446	0.05	66/199	13.18%
10	Androgen Response	-0.45156	-1.56892	0.006557	0.008377	0.05	21/96	9.06%
12	Interferon Alpha Response	-0.4253	-1.47311	0.016694	0.016817	0.125	35/93	16.80%
13	Wnt-beta Catenin Signaling	-0.46487	-1.39303	0.056058	0.03391	0.254	18/40	15.61%
14	TGF-beta Signaling	0.397714	1.313159	0.069825	0.045323	0.268	okt-53	5.11%

Table S3.5 Overview of all synthesized proteins with their respective calculated and observed masses and retention times

Miniprotein	Sequence	Yield (%)	Molecular weight calculated	Molecular weight observed	LCMS method	Retention time (min)	Observed ions
MiniMYC 1	(AcATEENVKRRTHNVLERQRRNELKRSFFG)$_2$K	16%	7137.1	3736.5	B	2.023	1190.3, 1020.4, 893.1, 793.9, 714.6, 649.7, 595.7, 549.9, 510.7, 476.7
MiniMYC, monomer 2	AcATEENVKRRTHNVLERQRRNELKRSCFA	16%	3483.0	3482.1	B	1.895	1161.5, 871.7, 697.5, 581.4, 498.5, 436.2
MiniMYC 3	(AcATEENVKRRTHNVLERQRRNELKRSSCFA)$_2$-Linker	31%	7260	7259.4	B	2.125	1210.9, 1038.1, 908.3, 807.5, 726.9, 660.9, 605.9, 559.4, 519.5
MonoMYC 4	AcATEENVKRRTHNVLERQRRNELKRSFFALRDQIPELEN-NEKAPKVVILKKATAYILSCA	0.5%	6978.1	6977.5	B	2.641	1396.6, 1163.8, 997.8, 873.1, 776.2, 698.7, 635.3,
DuoMYC 5	(AcATEENVKRRTHNVLERQRRNELKRSFFALRDQIPELEN-NEKAPKVVILKKATAYILSCA)$_2$-linker	23%	14134	14133	B	2.897	1414.28, 1285.8, 1178.7, 1088.1, 1010.6, 943.2, 884.4, 832.4, 786.3, 744.9, 707.7, 674.0, 643.4
MonoMYC 6	AcVKRRTHNVLERQRRNELKRSFFALRDQIPELENNEKAPKV-VILKKATAYILSVA$_\beta$C	6%	6532.7	6531.6	B	2.586	1089.5, 934.0, 817.4, 726.7, 649.0, 594.4
DuoMYC 7	(AcVKRRTHNVLERQRRNELKRSFFALRDQIPELENNEKAP-KVVILKKATAYILSA$_\beta$C)$_2$-linker	12%	13359	13358	B	2.888	1114.0, 1028.5, 955.1, 891.1, 835.9, 786.8, 743.1, 704.1, 668.9, 637.1, 608.2, 581.7, 557.6
FITC labeled DuoMYC 8	(AcATEENVKRRTHNVLERQRRNELKRSFFALRDQIPELEN-NEKAPKVVILKKATAYILSCA)$_2$-linker + 1/2/3 FITC	80%	1x FITC: 14524 2x FITC: 14913 3x FITC: 15303	1x FITC: 14523 2xFITC: 14913 3xFITC: 15301	B	2.942	1xFITC: 1453.39, 1321.35, 1211.26, 1118.14, 1038.41, 969.12, 908.75, 855.23, 807.03, 765.41, 727.19, 692.52 2xFITC: 1492.19, 1356.72, 1243.74, 1147.99, 1066.21, 995.13, 933.06, 878.17, 829.44, 785.89, 746.60, 711.19 3xFITC: 1392.27, 1276.16, 1178.11, 1093.99, 1021.20, 957.37, 901.11, 851.00, 806.37, 765.47
FITC-labelled Omomyc 9	AMADIGSMATEENVKRRTHNVLERQRRNELKRSFFALRD-QIPELENNEKAPKVVILKKATAYILSVQAETQKLISEIDLL-RKQNEQLKHKLEQLRNSCA +1/2/3/4x FITC	20%	1xFITC: 11917 2XFITC: 12306 3XFITC: 12695 4xFITC: 13085	1xFITC: 11916 2XFITC: 12306 3xFITC: 12695 4xFITC: 13084	B	3.3	1xFITC: 1324.92, 1190.49, 1084.30, 994.11, 917.56, 852.09, 794.42, 747.73 2xFITC: 1368.26, 1231.53, 1119.76, 1026.44, 947.64, 879.95, 821.36, 770.15. 724.84, 684.20 3xFITC: 1411.48, 1270.54, 1155.94, 1058.95, 977.57, 907.74, 847.42, 794.40, 747.72, 706.24, 669.18 4xFITC: 1454.82, 1309.44, 1190.49, 1091.37, 1007.49, 935.60, 873.29, 818.71, 770.67, 727.91